Boost-Up Efficiency of Defective Solar Panel Detection With Pre-Trained Attention Recycling

YeongHyeon Park [1,2], Myung Jin Kim [2], Uju Gim [2], Juneho Yi [1]

Department of Electrical and Computer Engineering, Sungkyunkwan University [1]

IoT Solution Business Group, SK Planet Co., Ltd. [2]

IEEE TRANSACTIONS ON INDUSTRY APPLICATIONS

Motivation

- ❑ Solar panel defects significantly degrade energy conversion efficiency [1,2]
- ❑ It is necessary to develop a practically deployable method 🧐
  - To solve real-world problems
  - To avoid blindly employing end-to-end deep learning methods

[1] A. Taşçıoğlu et al., "A power case study for monocrystalline and polycrystalline solar panels in Bursa city, Turkey," *International Journal of Photoenergy*, 2016
[2] S. Deitsch et al., "Automatic classification of defective photovoltaic module cells in electroluminescence images," *Solar Energy*, 2019

Key idea

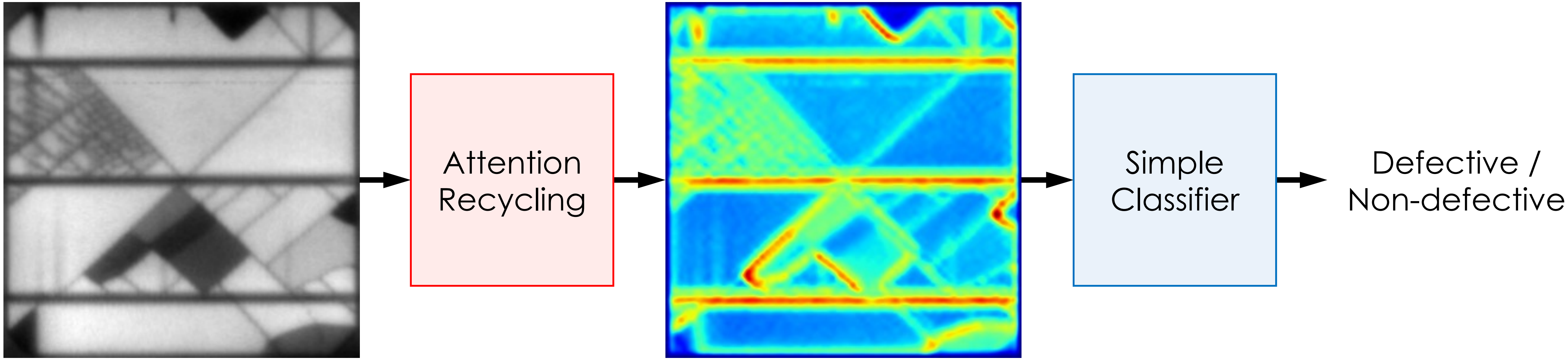

Recycling of a pre-trained attention mechanism

Boost-Up Efficiency of Defective Solar Panel Detection With Pre-Trained Attention Recycling

Details

Anomaly Detection

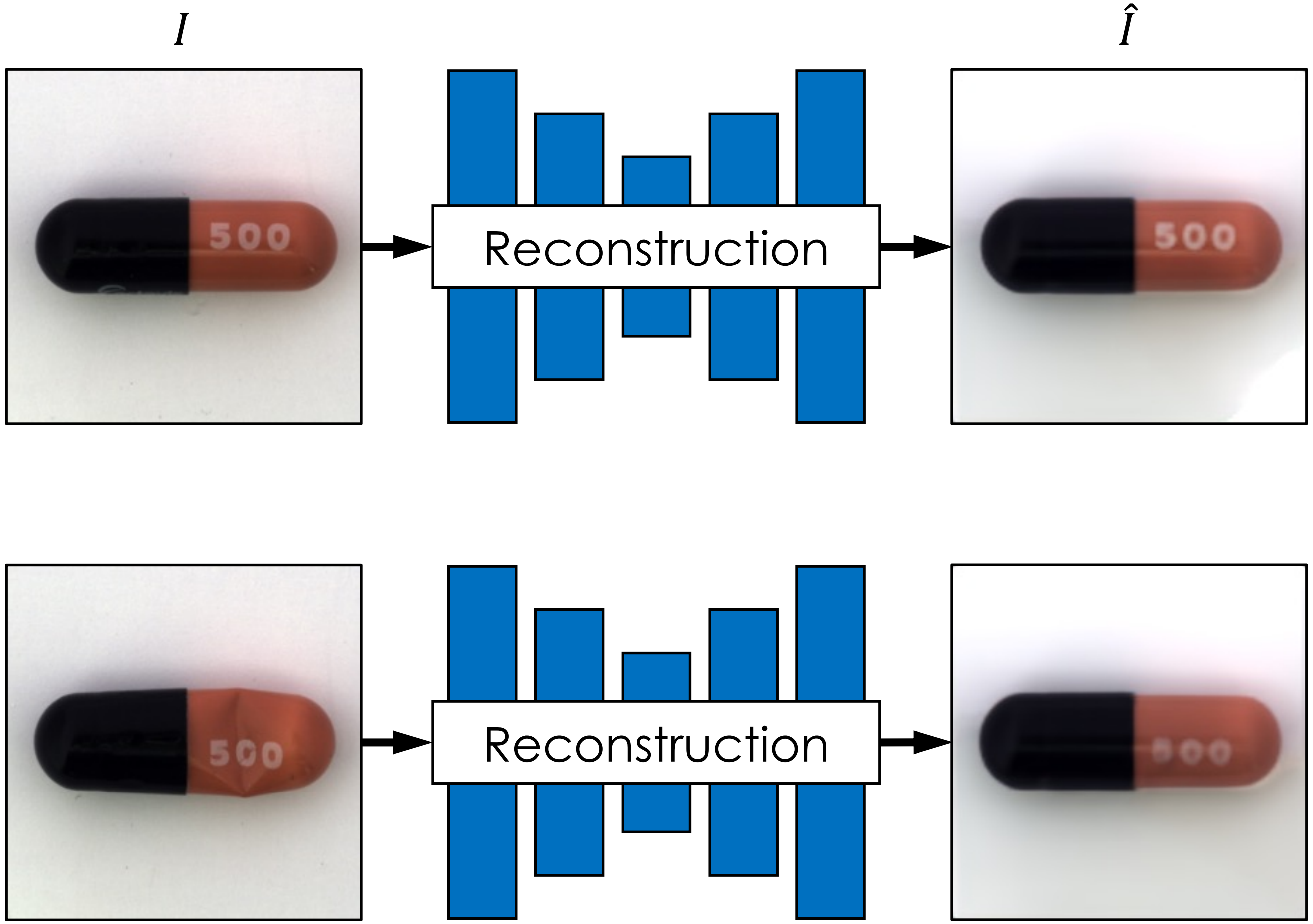

[3] Y. Park et al., “Neural Network Training Strategy to Enhance Anomaly Detection Performance: A Perspective on Reconstruction Loss Amplification,” *arXiv*, 2023

Anomaly Detection

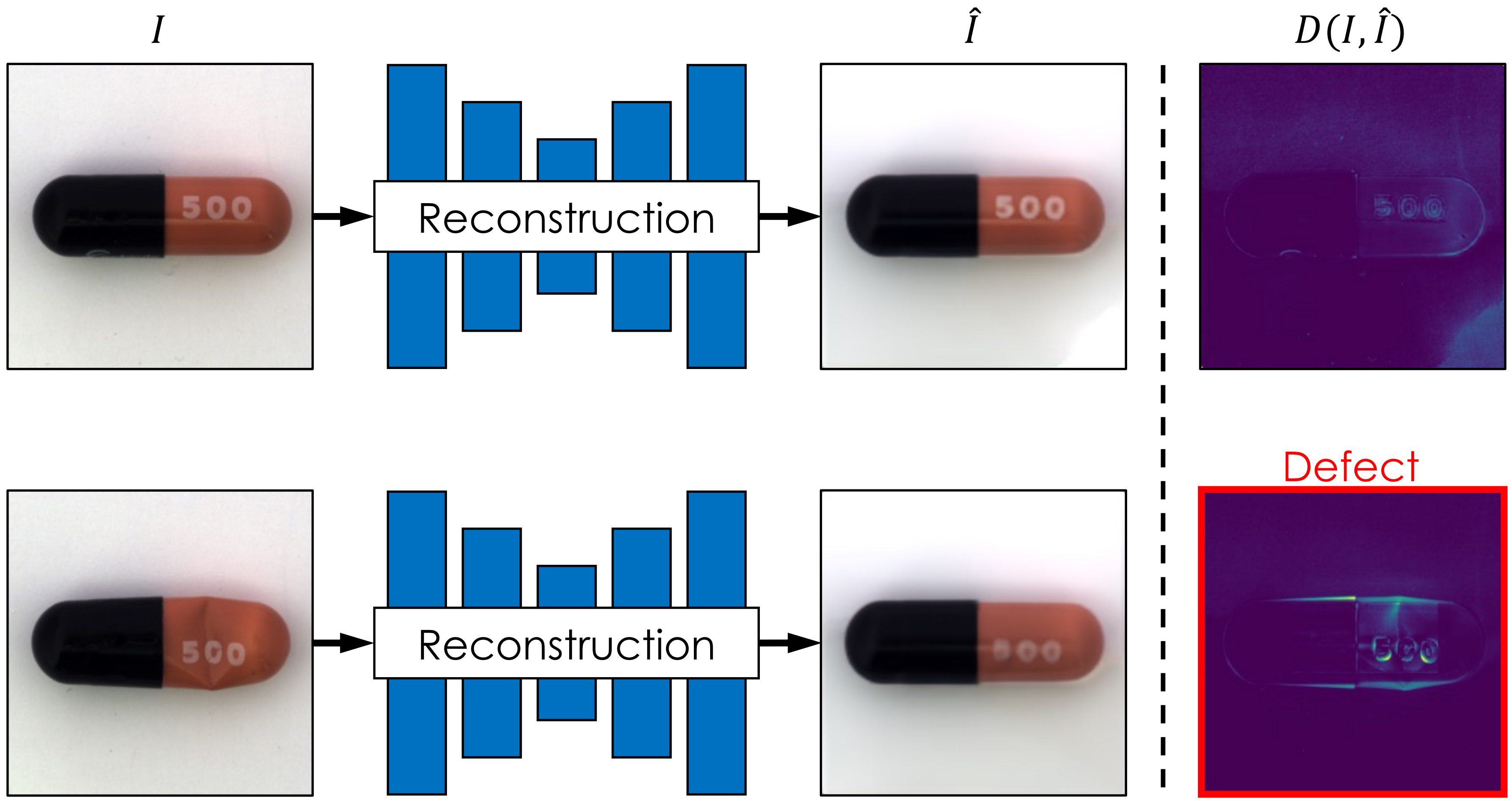

[3] Y. Park et al., "Neural Network Training Strategy to Enhance Anomaly Detection Performance: A Perspective on Reconstruction Loss Amplification," *arXiv*, 2023

Anomaly Detection

❑ Unsupervised anomaly detection based on reconstruction error

- \+ Eases class imbalance problem
- \+ Training with non-defective samples only
- – Deep neural networks consume lots of power
- – Requires a large-scale dataset

❑ Defective solar panel detection

- \+ Class balanced dataset
- \+ Easy to understand without deep knowledge
- – Small quantity of samples

[3] Y. Park et al., "Neural Network Training Strategy to Enhance Anomaly Detection Performance: A Perspective on Reconstruction Loss Amplification," *arXiv*, 2023

Solar panels [4]

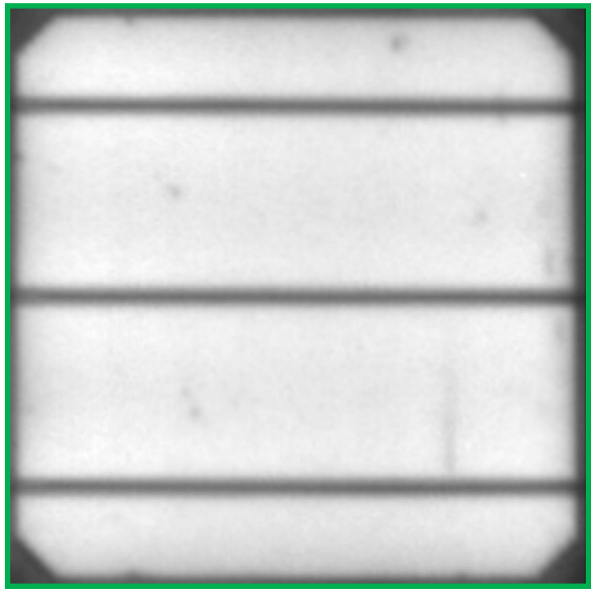

Non-defective

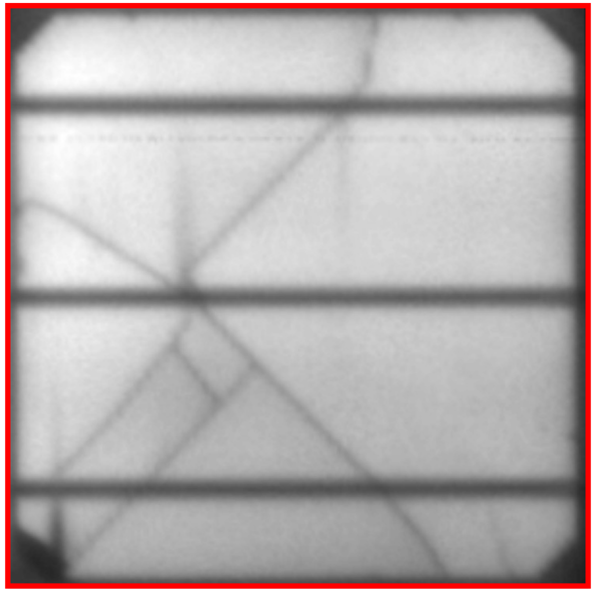

Defective
(Crack)

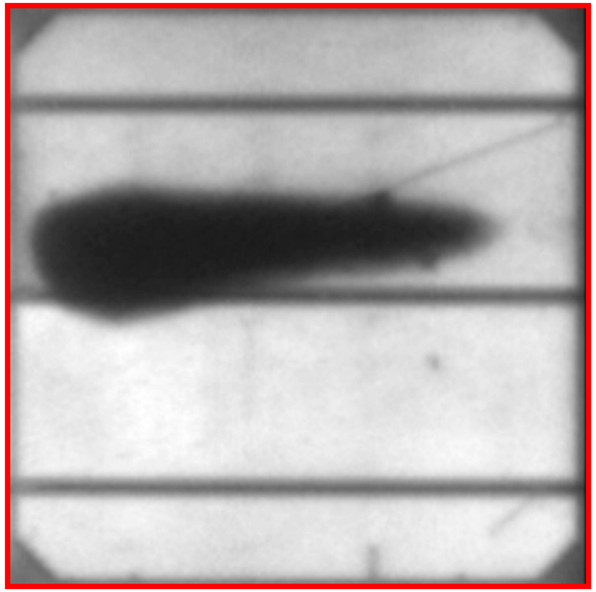

Defective
(Contamination)

[4] C. Buerhop-Lutz et al.,"A benchmark for visual identification of defective solar cells in electroluminescence imagery," EU PVSEC, 2018

Solar panels [4]

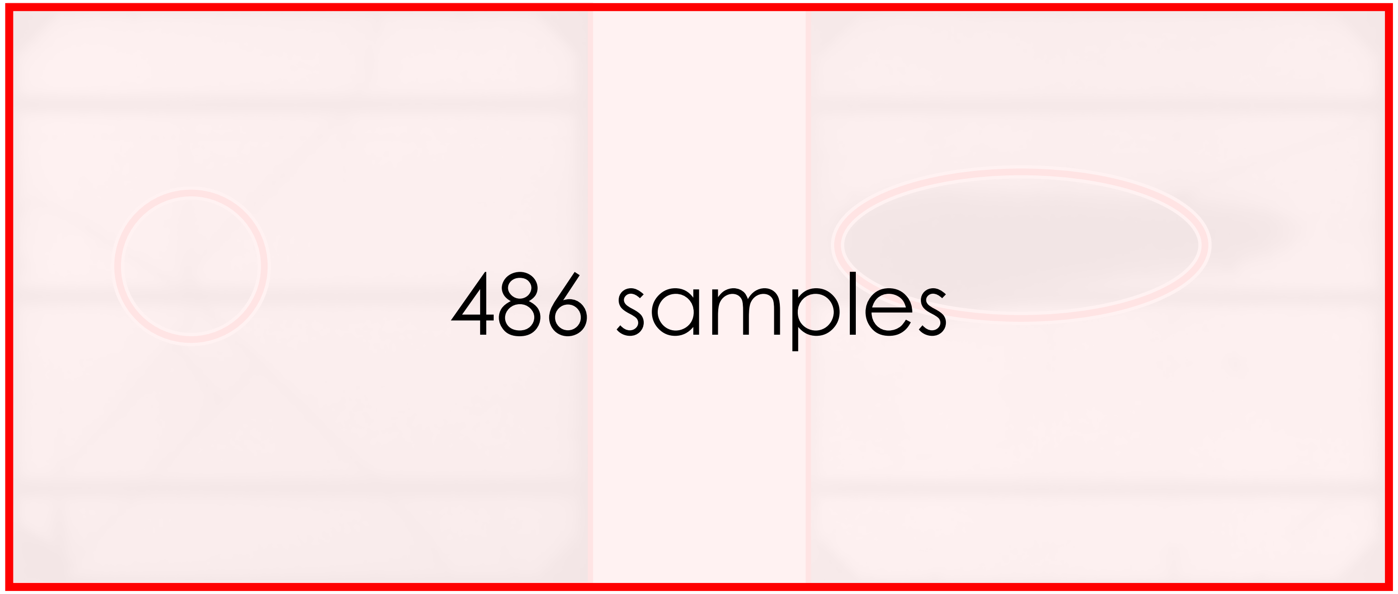

Balanced small dataset

[4] C. Buerhop-Lutz et al.,"A benchmark for visual identification of defective solar cells in electroluminescence imagery," EU PVSEC, 2018

Solar panels [4]

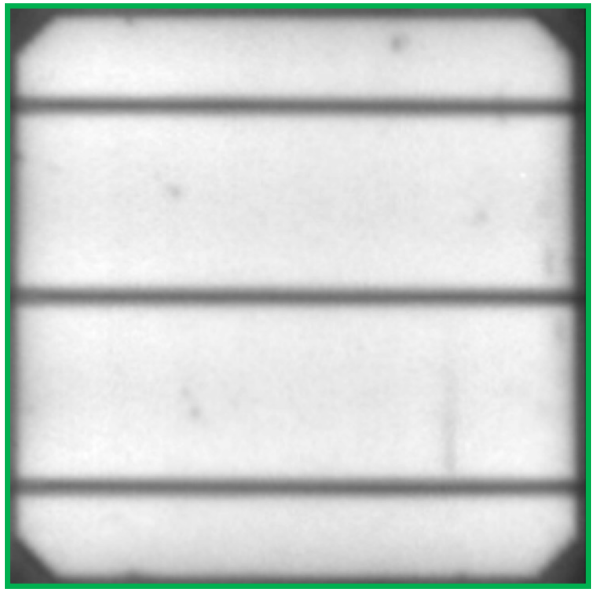

Non-defective

Faint

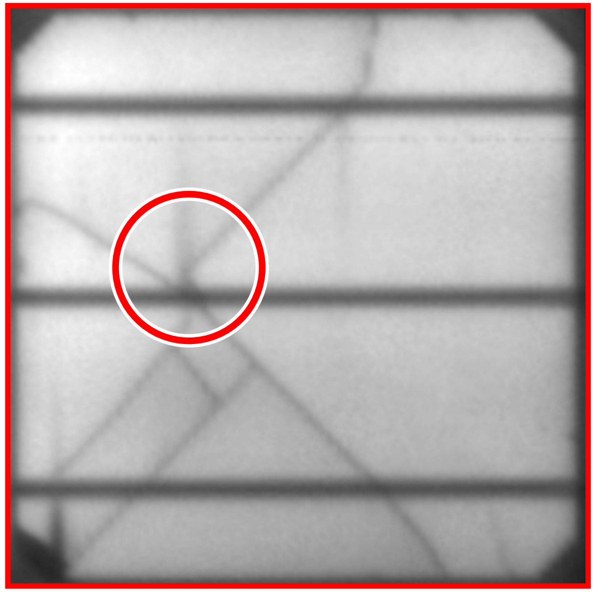

Defective
(Crack)

Smooth inside

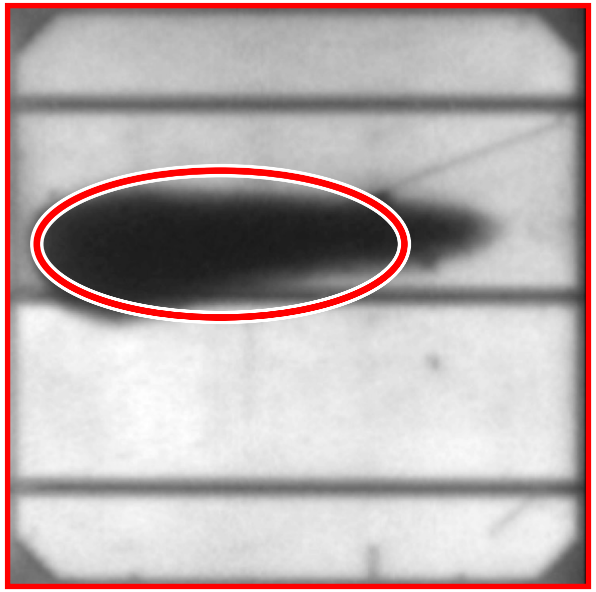

Defective
(Contamination)

[4] C. Buerhop-Lutz et al.,"A benchmark for visual identification of defective solar cells in electroluminescence imagery," EU PVSEC, 2018

Workflow

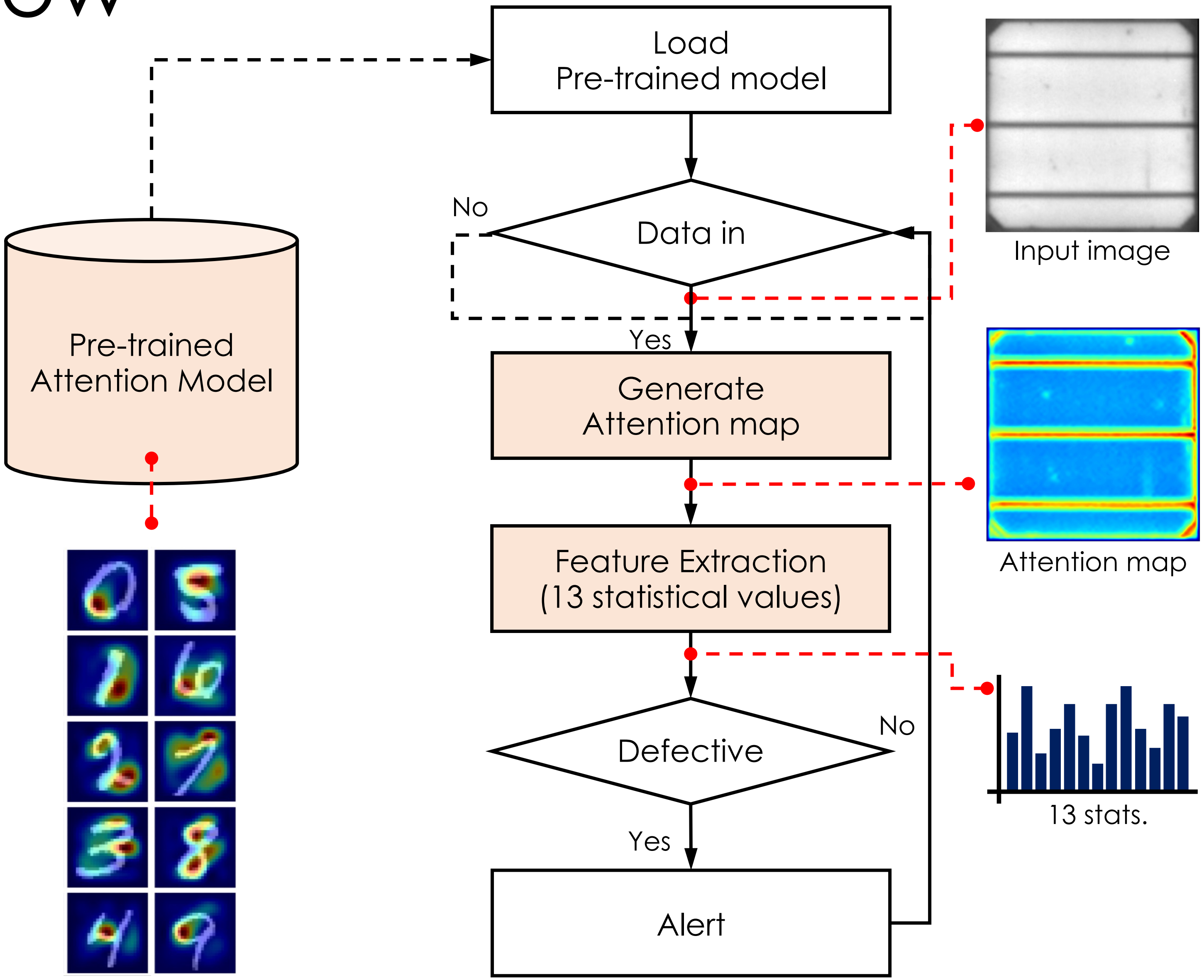
Load
Pre-trained model
Data in
No
Yes
Generate
Attention map
Feature Extraction
(13 statistical values)
Defective
No
Yes
Alert
Pre-trained
Attention Model
Input image
Attention map
13 stats.

Emphasizing the defect

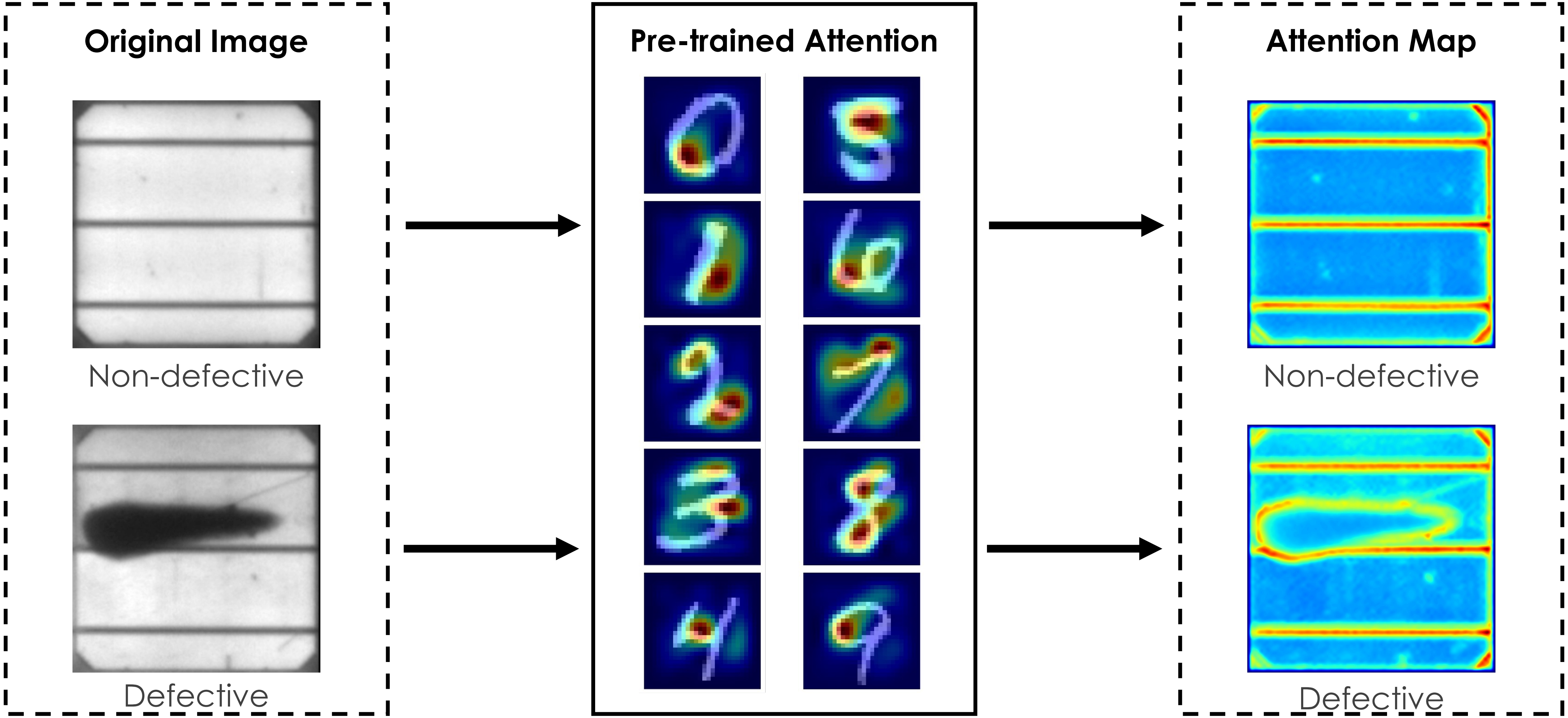

Emphasizing the defect

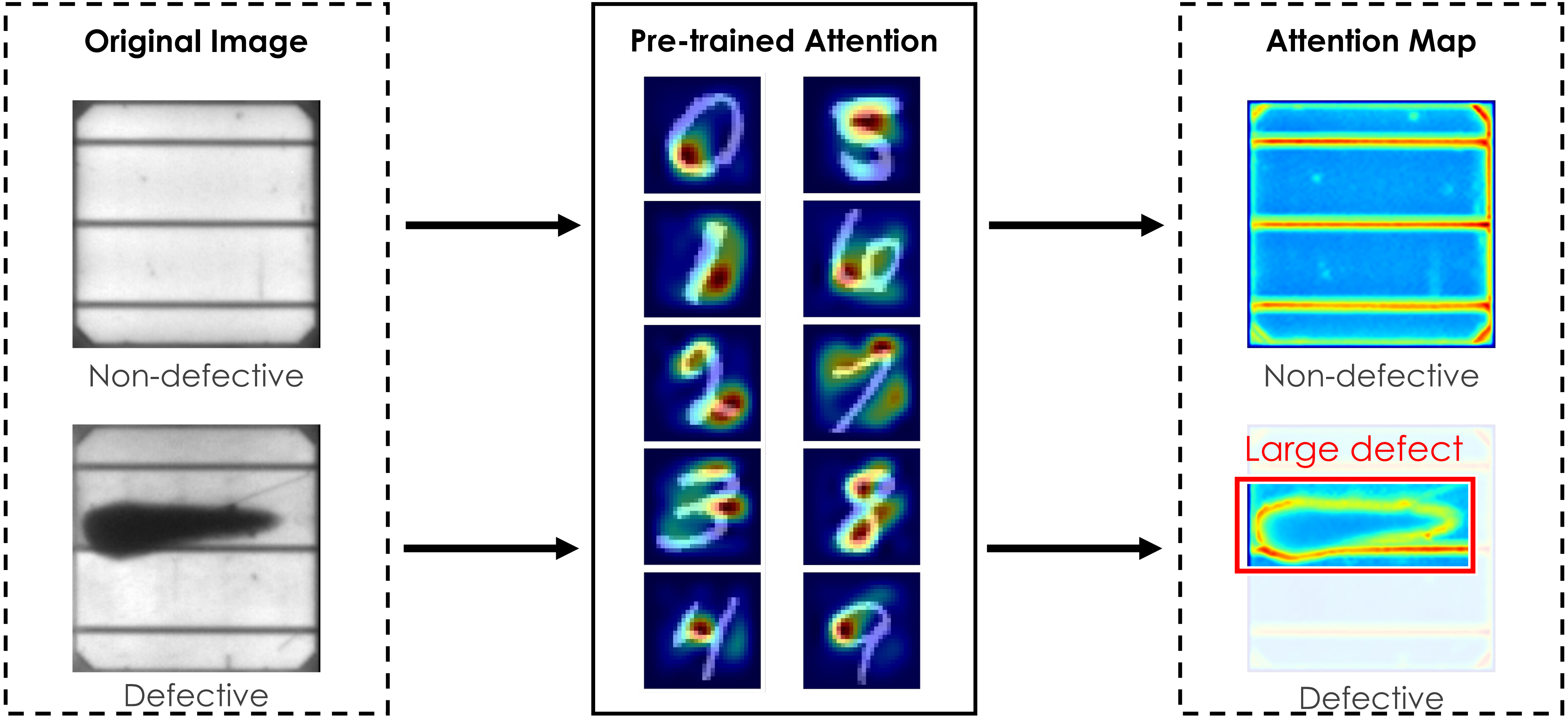

Emphasizing the defect

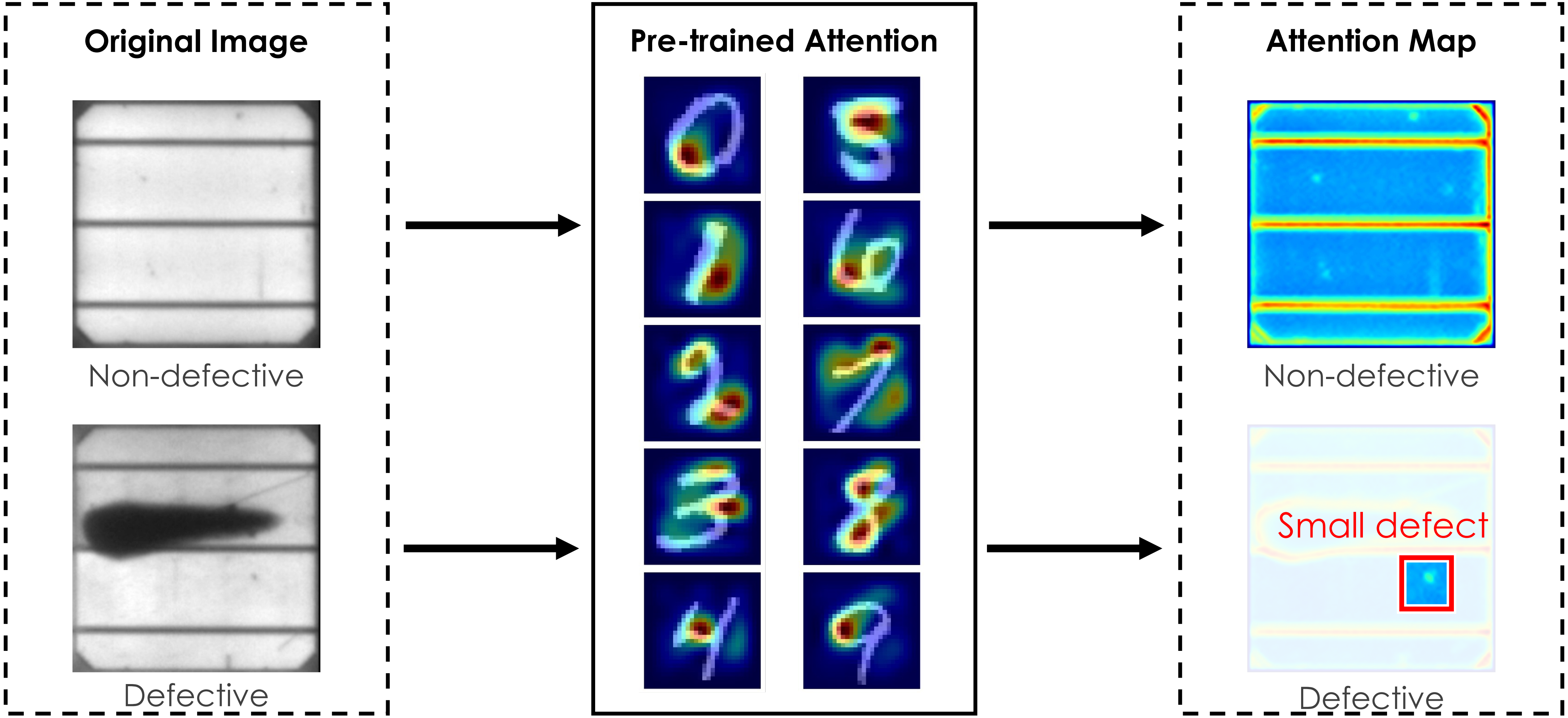

Statistical feature extraction

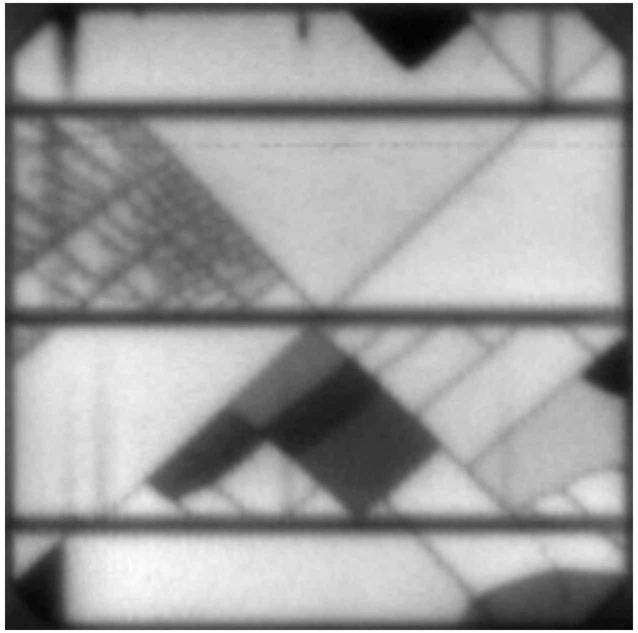

Feature	Description
$\mu_{img.}$	Mean of whole pixel values
$\sigma_{img.}$	Standard deviation (SD) of whole pixel values
R	Outlier rate that deviate from the threshold, $\mu \pm 1.5\sigma$, among image
$S(img.)$	Skewness of whole pixel values
$S(\mu_h)$	Skewness of the pixel mean along the height axis
$S(\mu_w)$	Skewness of the pixel mean along the width axis
$S(\sigma_h)$	Skewness of the pixel SD along the height axis
$S(\sigma_w)$	Skewness of the pixel SD along the width axis
$K(img.)$	Kurtosis of whole pixel values
$K(\mu_h)$	Kurtosis of the pixel mean along the height axis
$K(\mu_w)$	Kurtosis of the pixel mean along the width axis
$K(\sigma_h)$	Kurtosis of the pixel SD along the height axis
$K(\sigma_w)$	Kurtosis of the pixel SD along the width axis

Statistical feature extraction

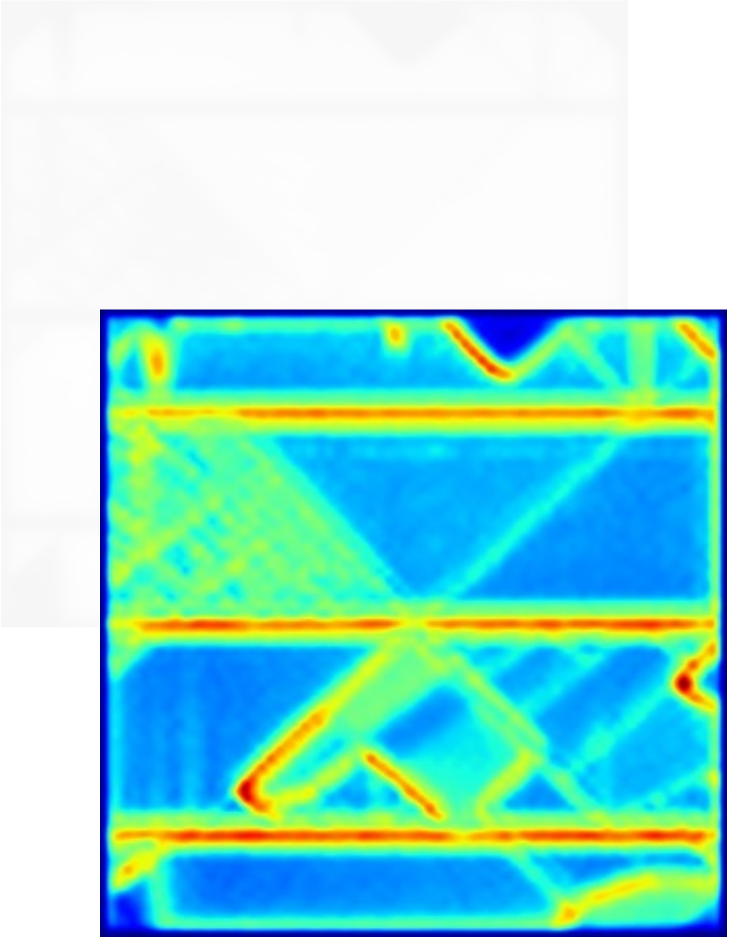

Feature	Description
$\mu_{img.}$	Mean of whole pixel values
$\sigma_{img.}$	Standard deviation (SD) of whole pixel values
R	Outlier rate that deviate from the threshold, $\mu \pm 1.5\sigma$, among image
$S(img.)$	Skewness of whole pixel values
$S(\mu_h)$	Skewness of the pixel mean along the height axis
$S(\mu_w)$	Skewness of the pixel mean along the width axis
$S(\sigma_h)$	Skewness of the pixel SD along the height axis
$S(\sigma_w)$	Skewness of the pixel SD along the width axis
$K(img.)$	Kurtosis of whole pixel values
$K(\mu_h)$	Kurtosis of the pixel mean along the height axis
$K(\mu_w)$	Kurtosis of the pixel mean along the width axis
$K(\sigma_h)$	Kurtosis of the pixel SD along the height axis
$K(\sigma_w)$	Kurtosis of the pixel SD along the width axis

Statistical feature extraction

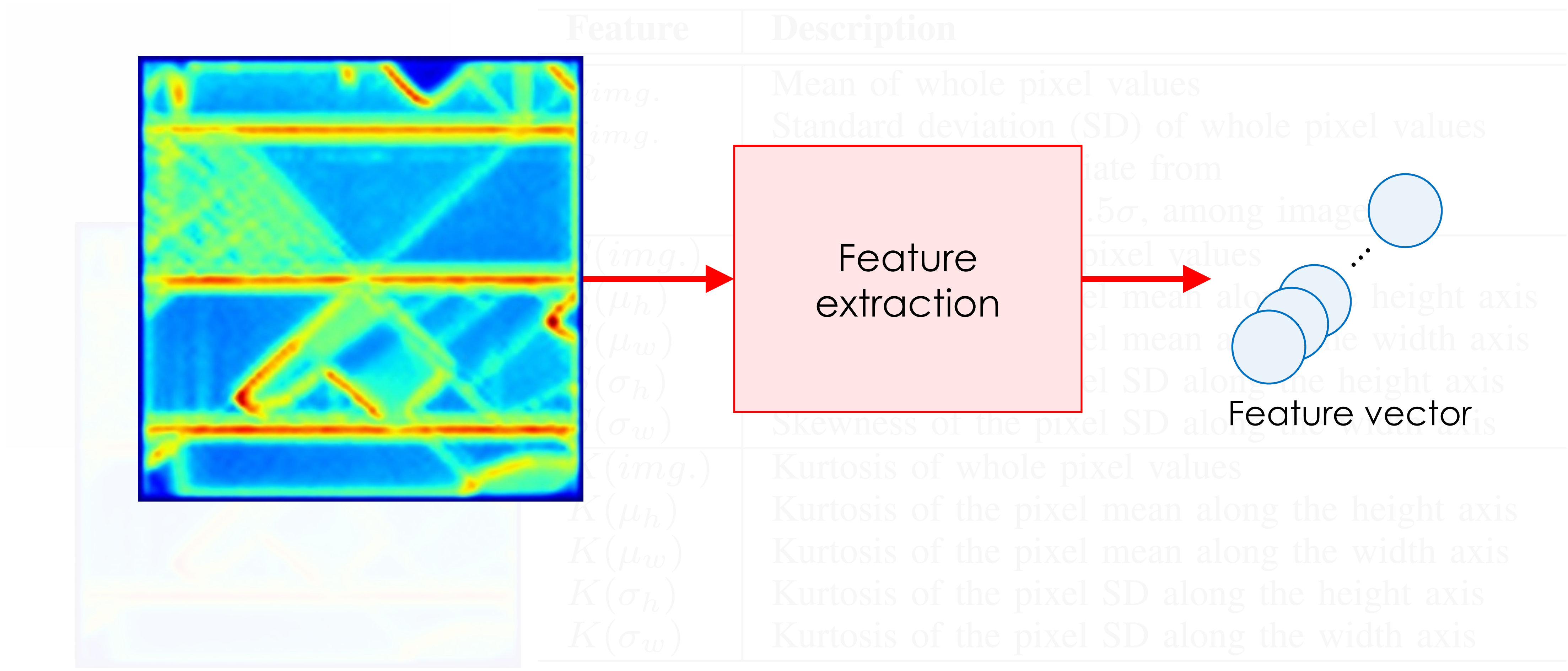

Pre-trained attention

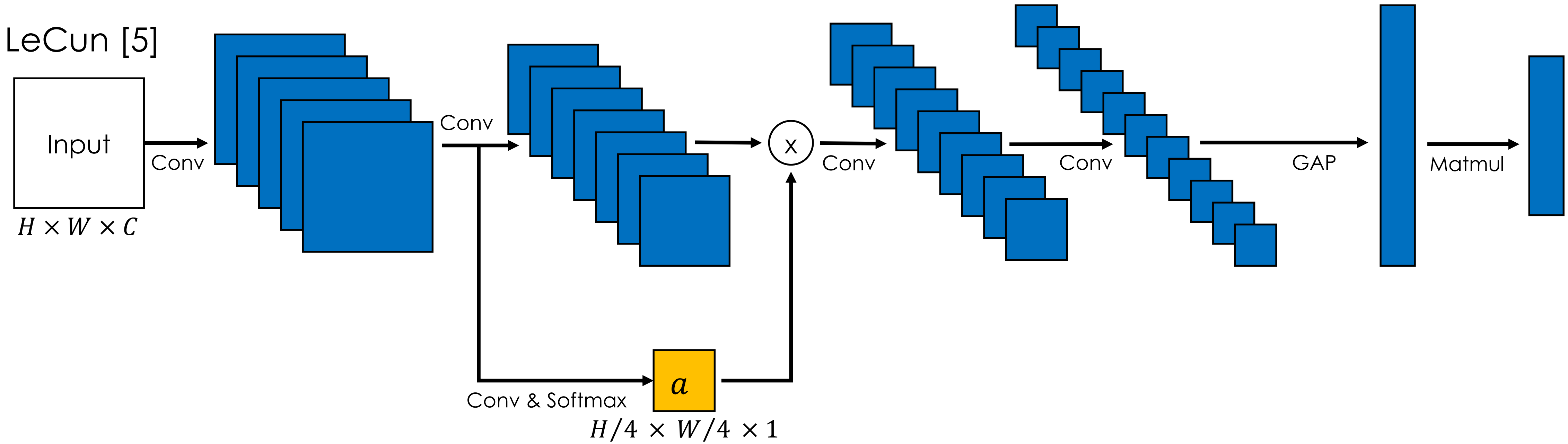

[5] Y. LeCun, et al. "Gradient-based learning applied to document recognition." Proceedings of the IEEE, 1998

Pre-trained attention

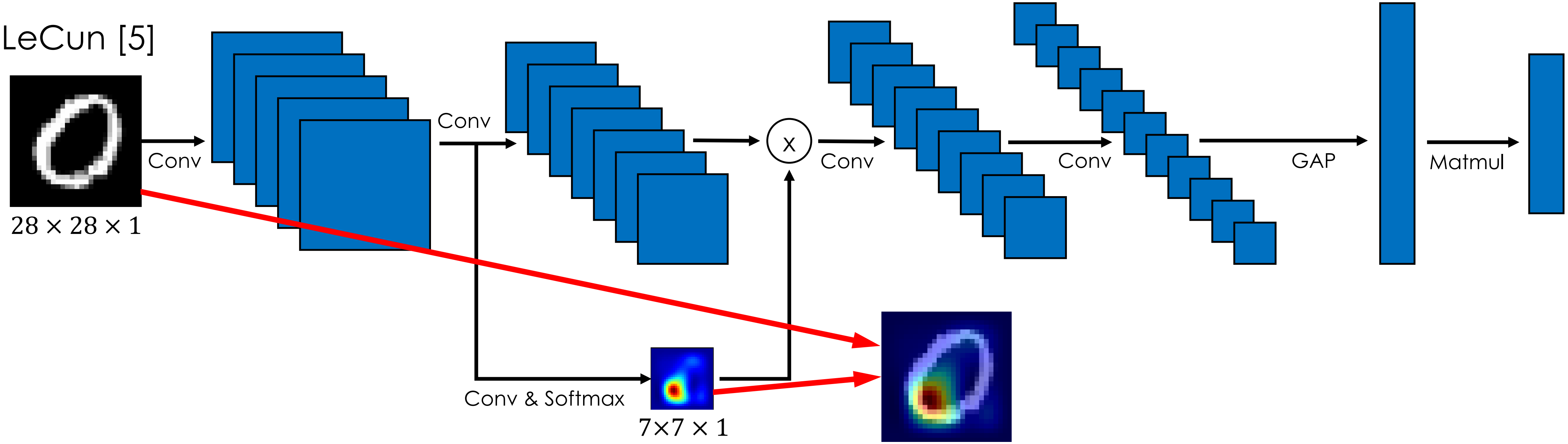

[5] Y. LeCun, et al. “Gradient-based learning applied to document recognition.” Proceedings of the IEEE, 1998

Pre-trained attention

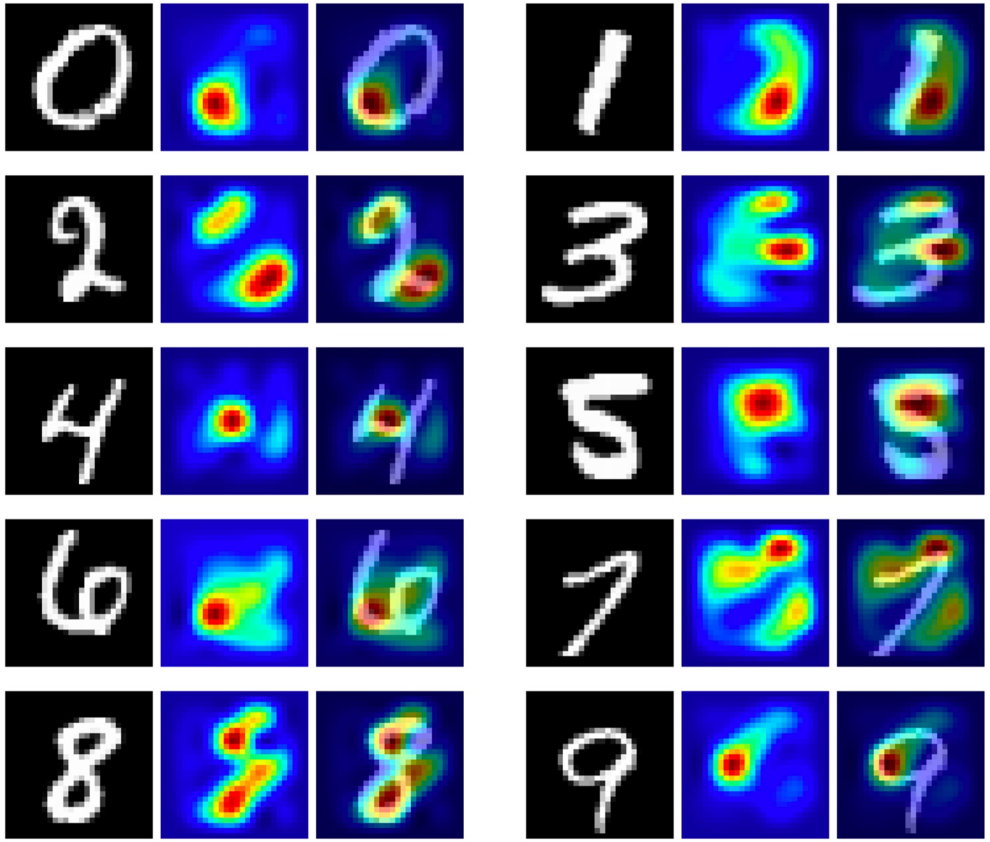

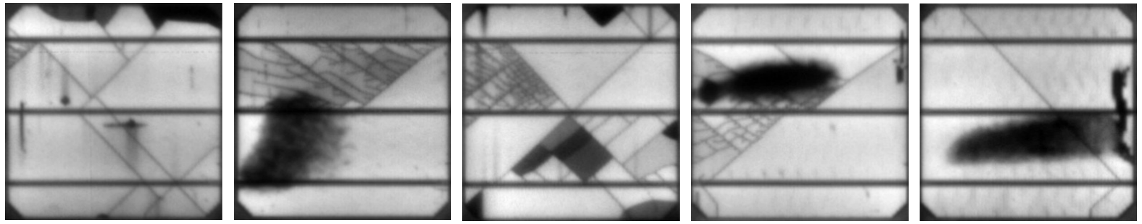

[5] Y. LeCun, et al. “Gradient-based learning applied to document recognition.” Proceedings of the IEEE, 1998

Pre-trained attention

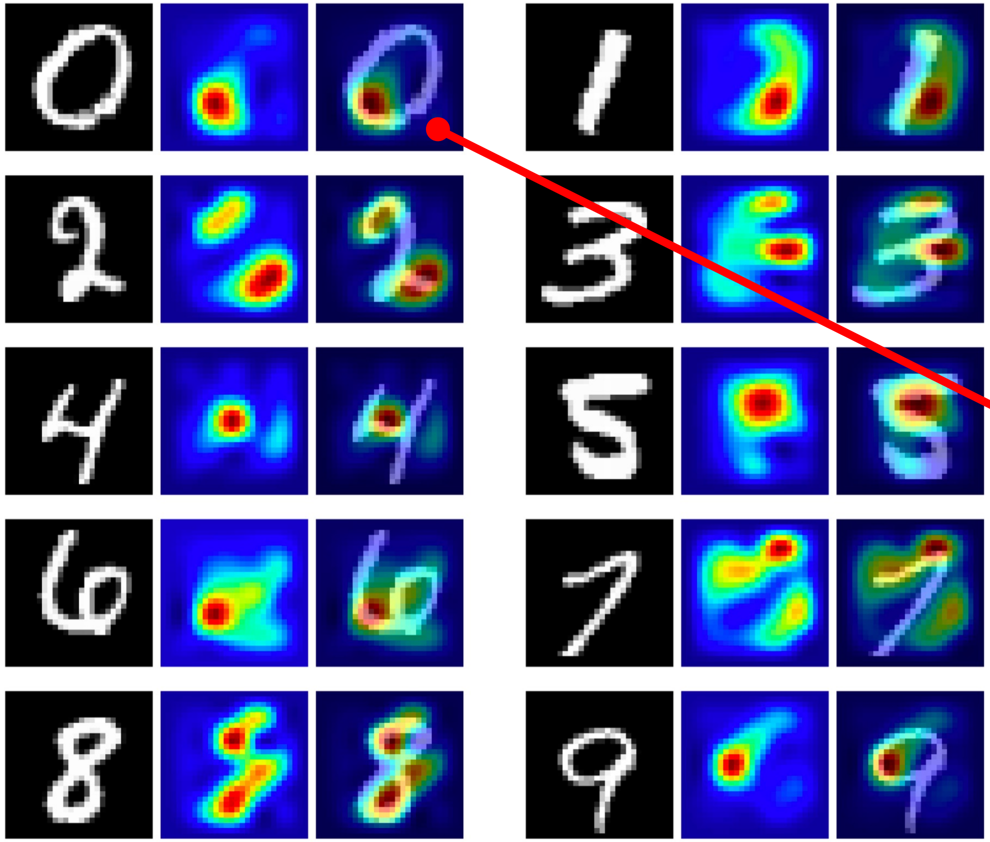

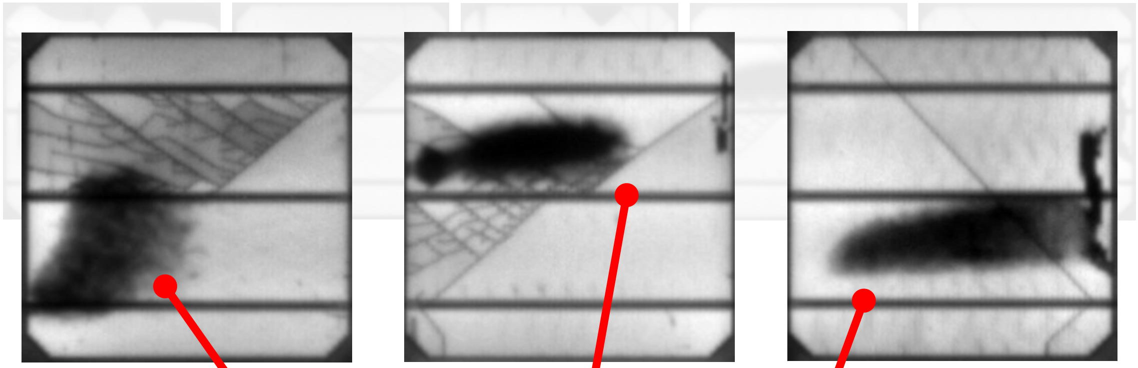

Stroke bends

[5] Y. LeCun, et al. "Gradient-based learning applied to document recognition." Proceedings of the IEEE, 1998

Pre-trained attention

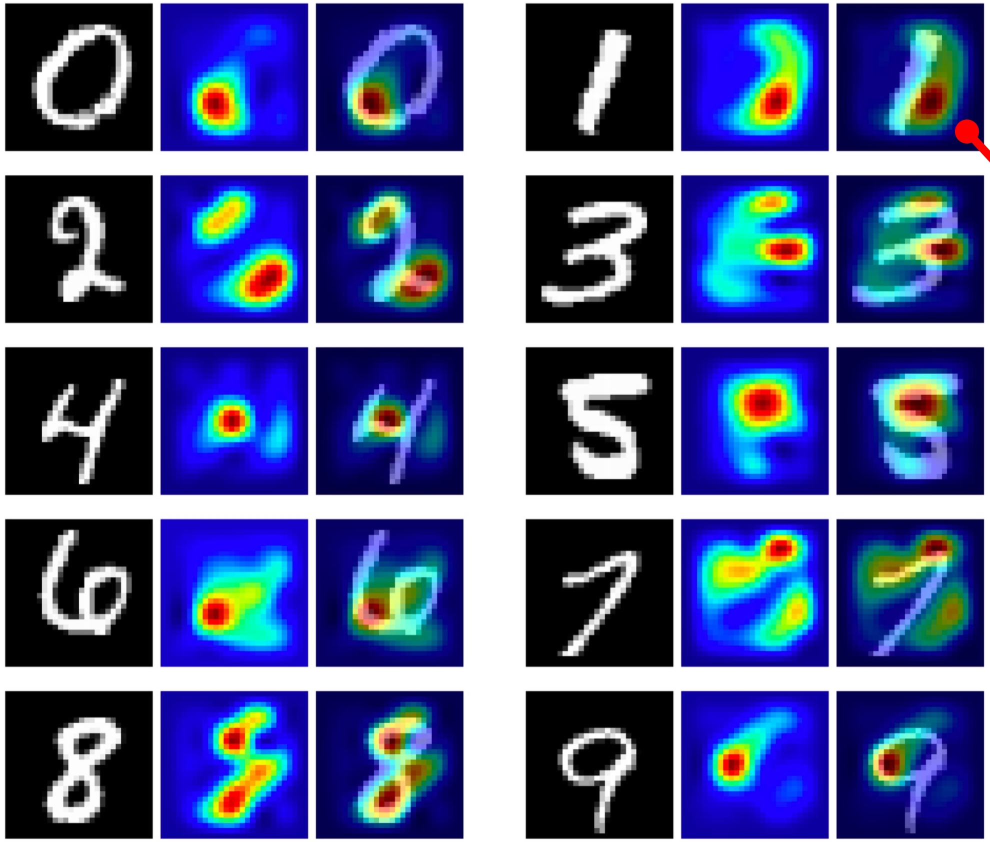

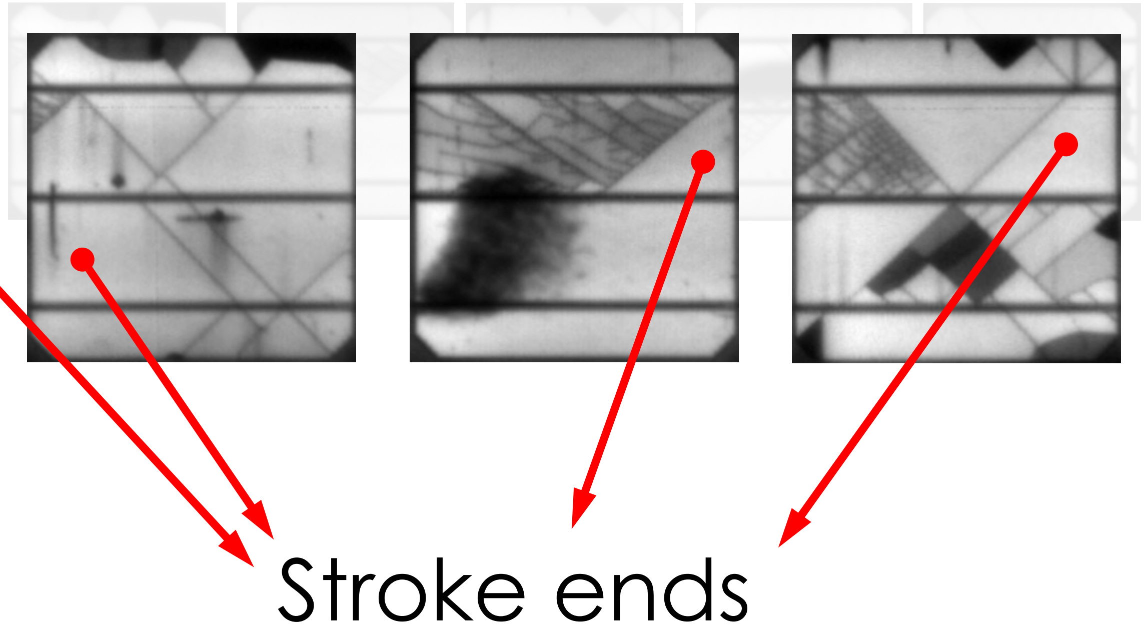

[5] Y. LeCun, et al. "Gradient-based learning applied to document recognition." Proceedings of the IEEE, 1998

Pre-trained attention

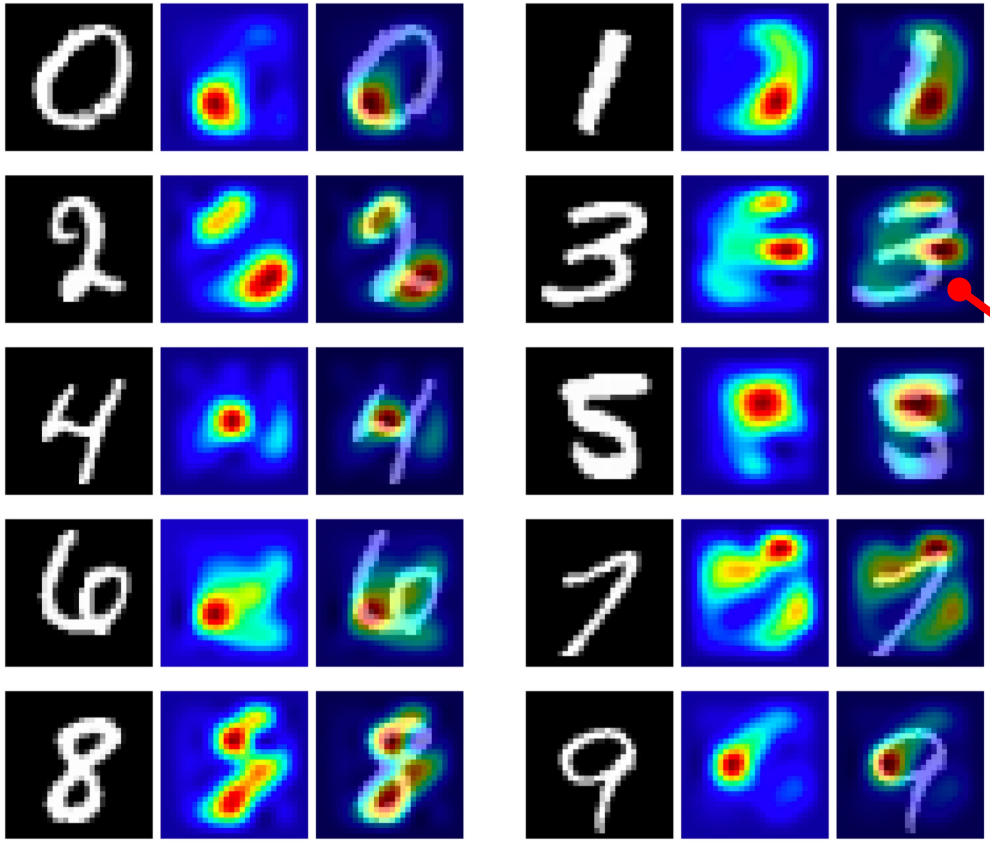

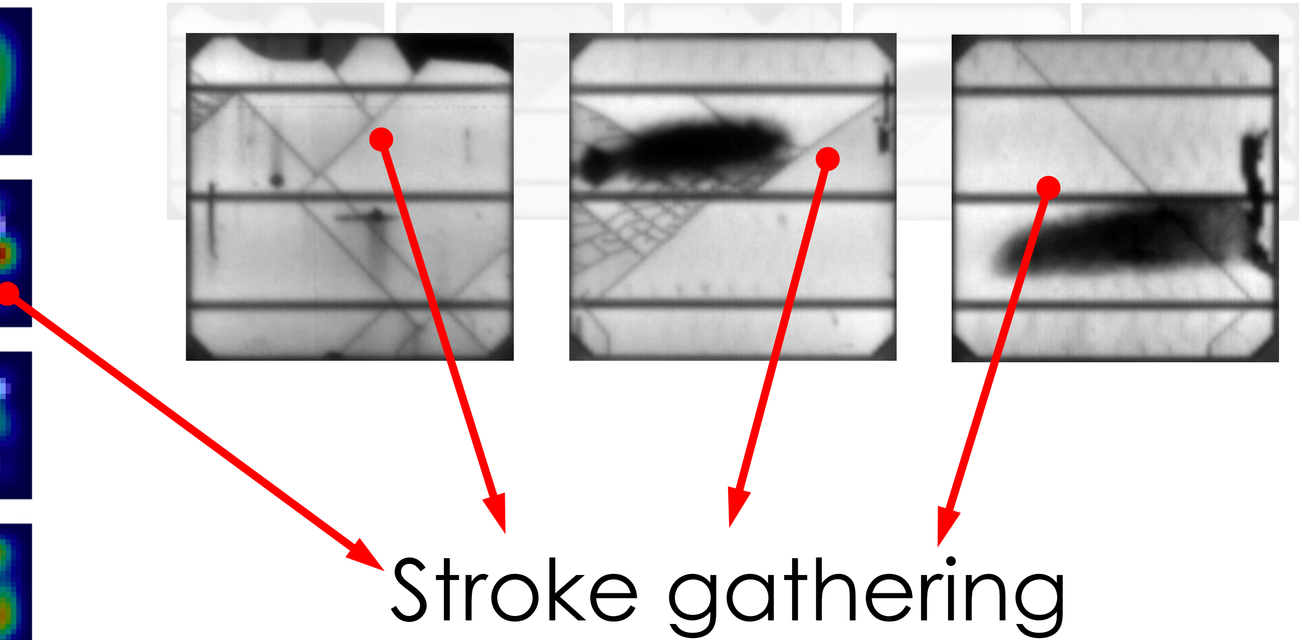

[5] Y. LeCun, et al. "Gradient-based learning applied to document recognition." Proceedings of the IEEE, 1998

Pre-trained attention

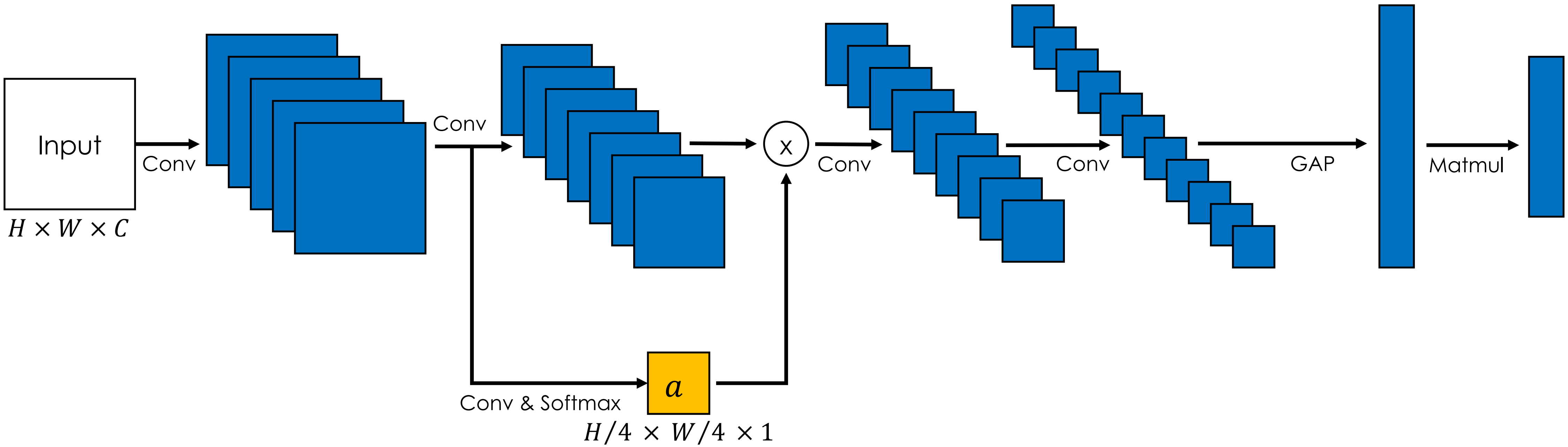

Pre-trained attention

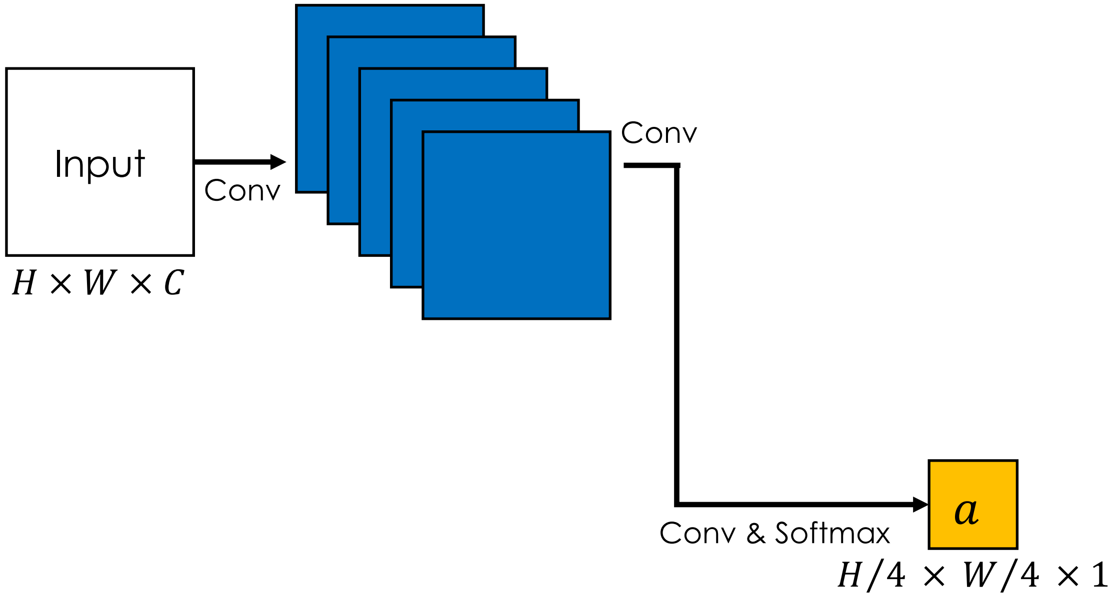

Pre-trained attention

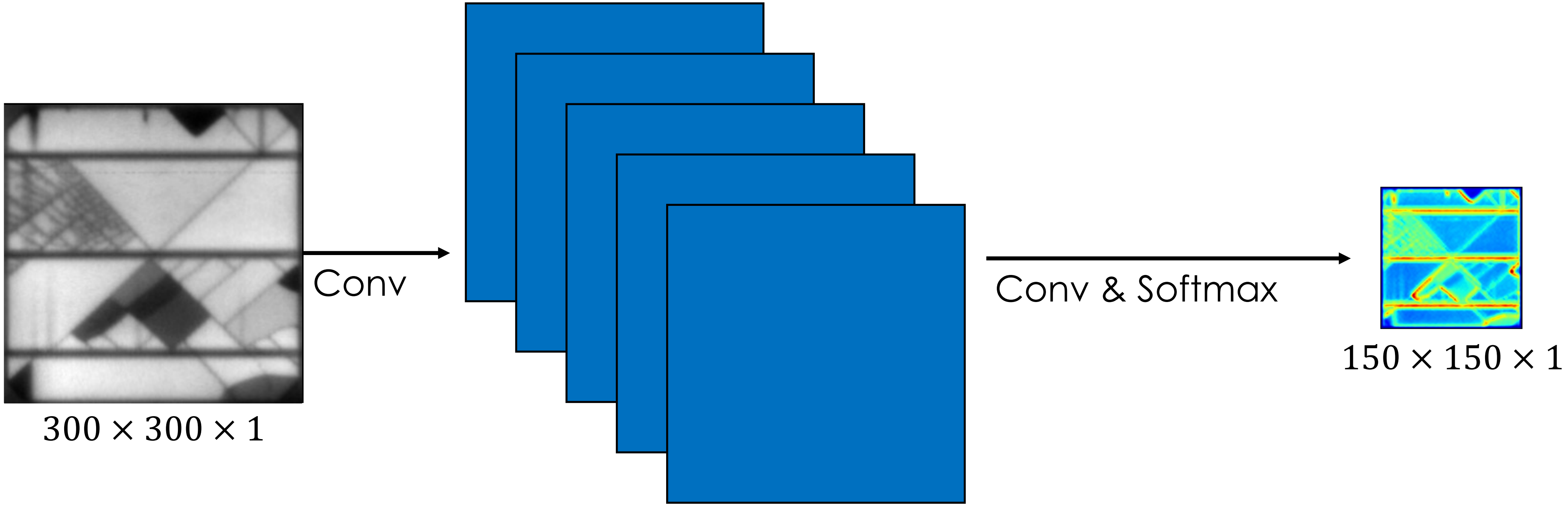

Experiments: dataset [4]

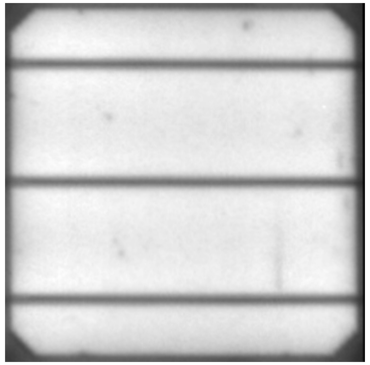

Non-defective

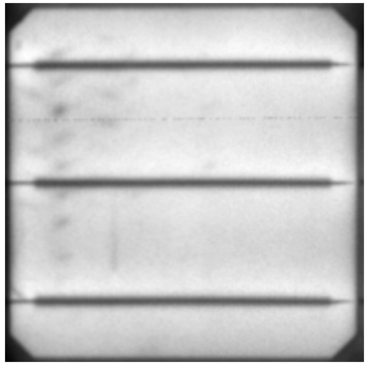

Defective
(1/3-level)

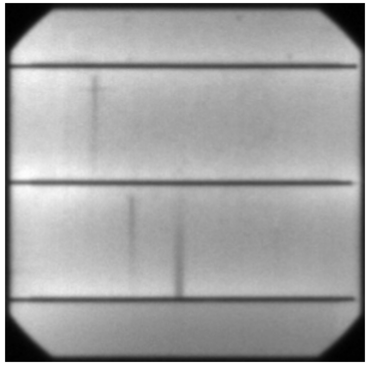

Defective
(2/3-level)

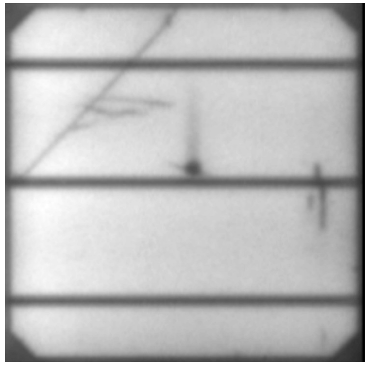

Defective
(Crack)

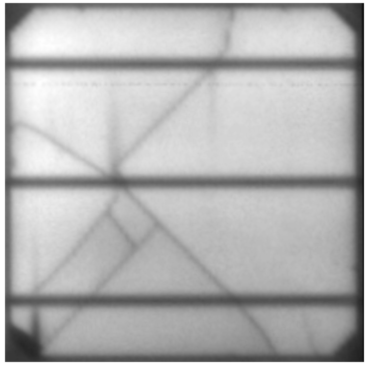

Defective
(Crack)

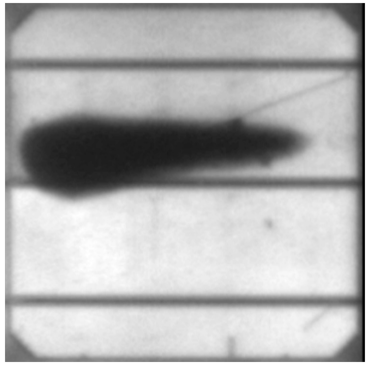

Defective
(Contamination)

[4] C. Buerhop-Lutz et al.,"A benchmark for visual identification of defective solar cells in electroluminescence imagery," EU PVSEC, 2018

Experiments: dataset [4]

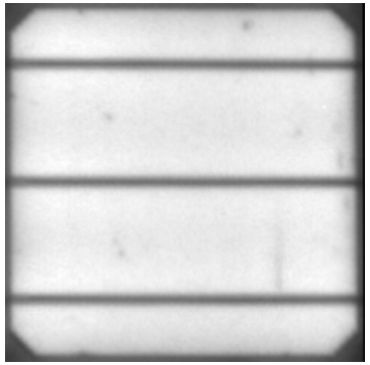

Non-defective

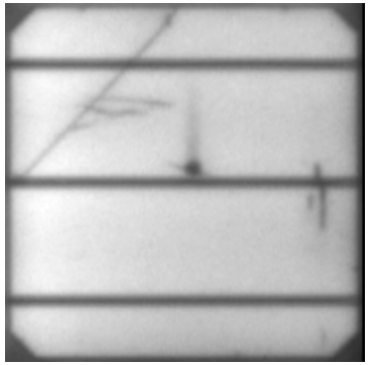

Defective
(Crack)

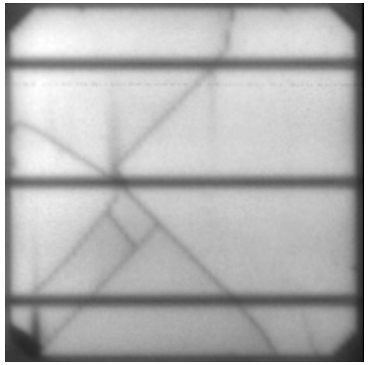

Defective
(Crack)

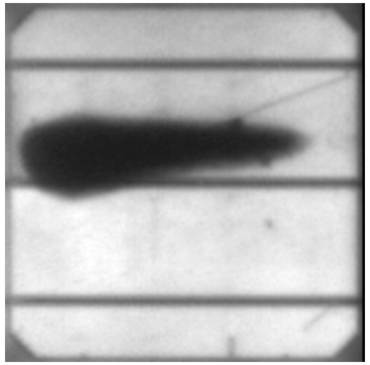

Defective
(Contamination)

Task-A

[4] C. Buerhop-Lutz et al.,"A benchmark for visual identification of defective solar cells in electroluminescence imagery," EU PVSEC, 2018

Experiments: dataset [4]

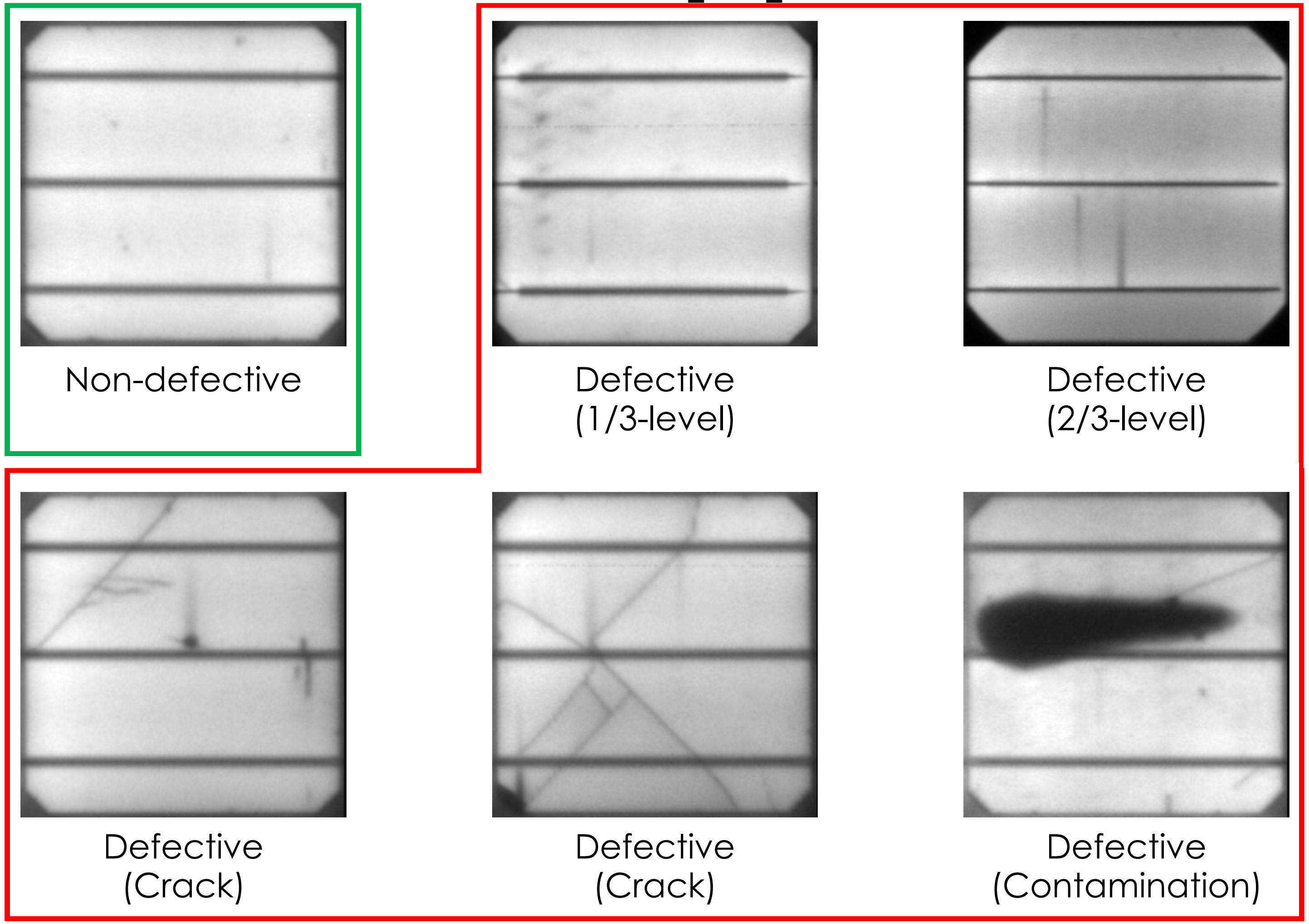

Task-B

[4] C. Buerhop-Lutz et al.,"A benchmark for visual identification of defective solar cells in electroluminescence imagery," EU PVSEC, 2018

Experiments: models

Thresholding model

- Rule: thresholding of extracted feature values

Machine learning models

- Decision Tree (DT) [6]
- Random Forest (RF) [7]
- eXtreme Gradient Boosting (XGB) [8]
- Light Gradient Boosting Machine (LGBM) [9]
- Support Vector Machine (SVM) [10]

Deep learning model

- EfficientNet-B0 (EffNetB0) [11]: end-to-end SOTA classification model

[6] B. Li et al., "Classification and regression trees," Biometrics, 1984
[7] T. K. Ho, "Random decision forests," ICDAR, 1995
[8] T. Chen et al., "XGBoost: A scalable tree boosting system," KDD, 2016
[9] G. Ke et al., "LightGBM: A highly efficient gradient boosting decision tree," NeurIPS, 2017
[10] C. Cortes et al., "Support-vector networks," Machine Learning, 1995
[11] M. Tan et al., "EfficientNet: Rethinking model scaling for convolutional neural networks," ICML, 2019

Attention on solar panels

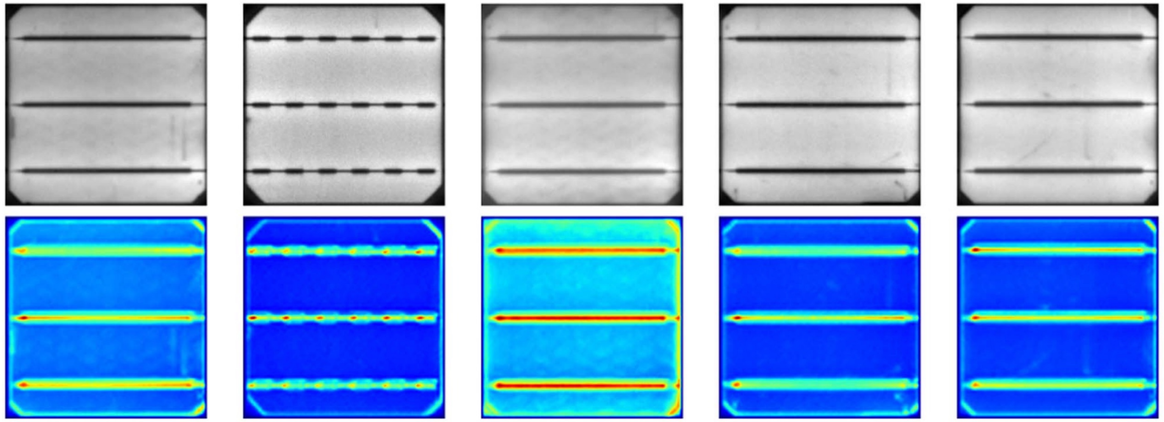

Non-defective

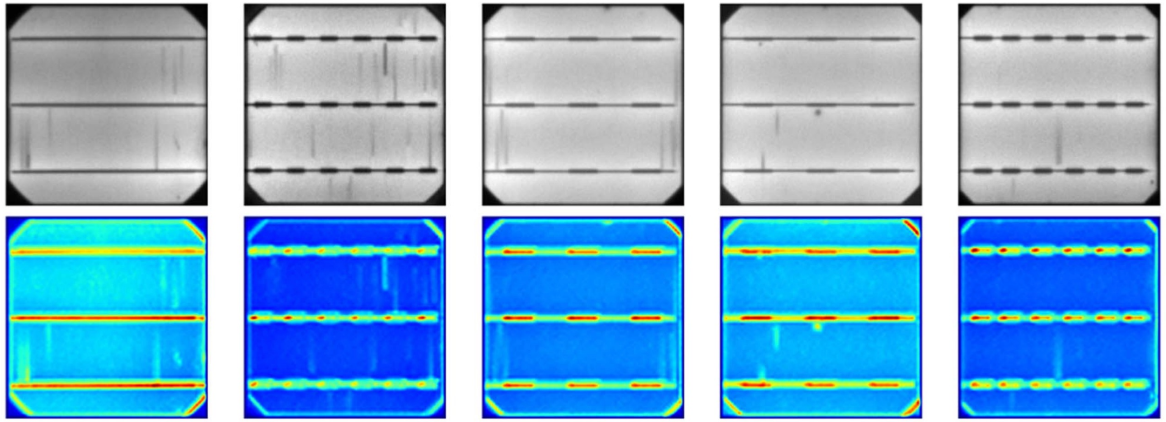

1/3-level defective

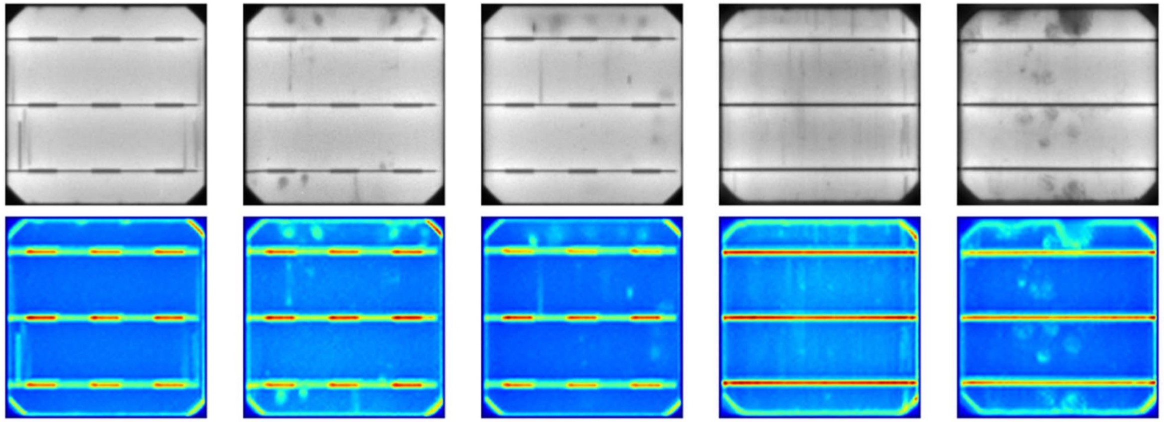

2/3-level defective

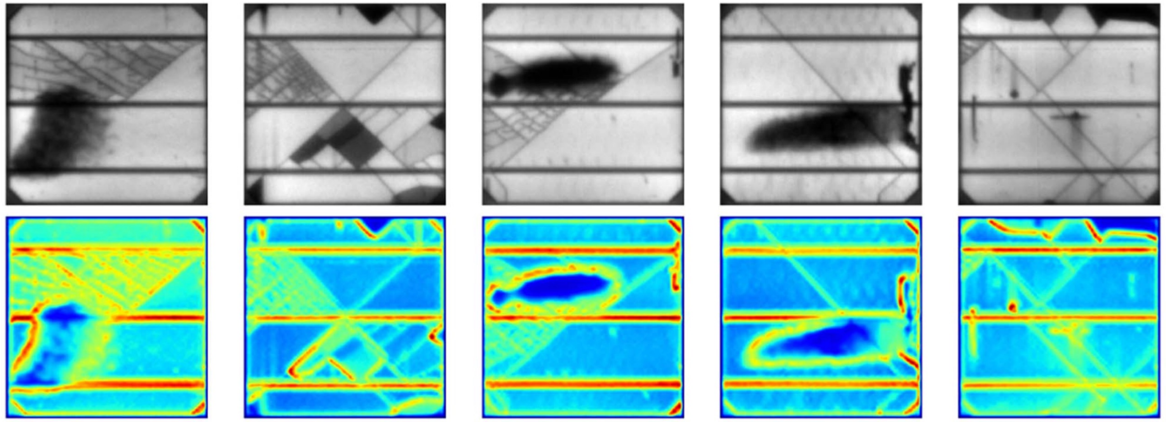

Absolute defective

Attention on solar panels

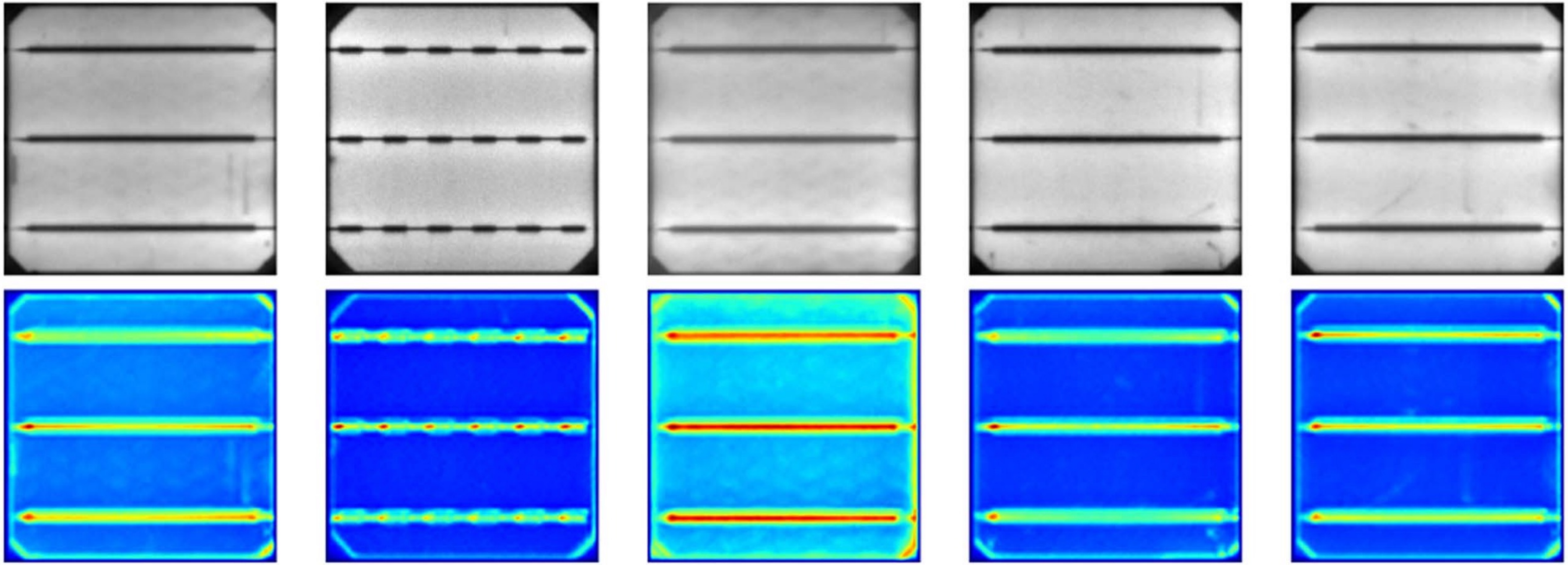

Non-defective

Attention on solar panels

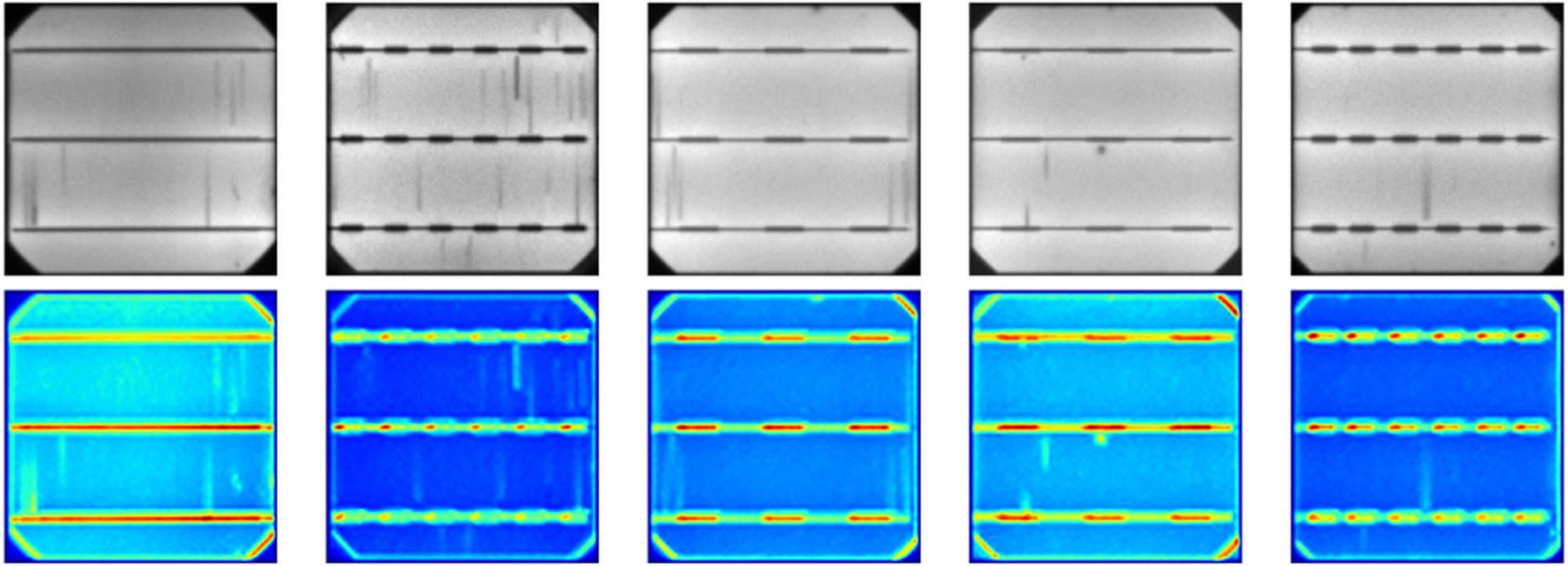

1/3-level defective

Attention on solar panels

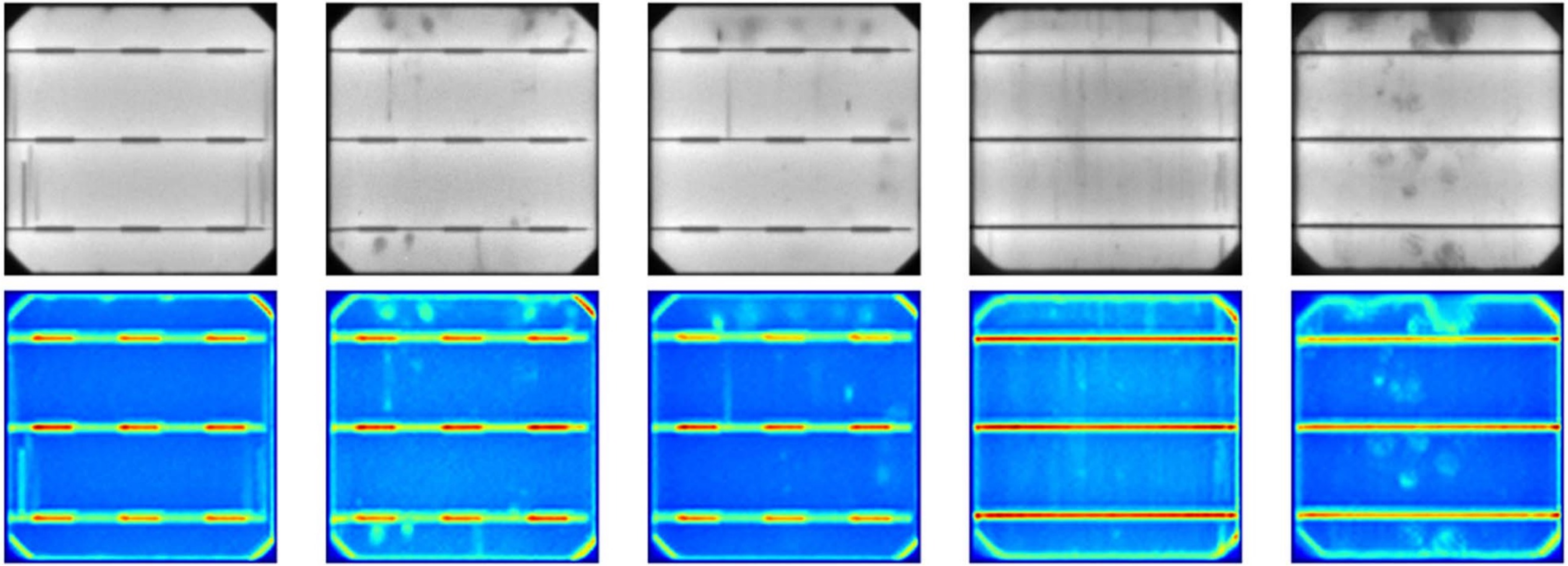

2/3-level defective

Attention on solar panels

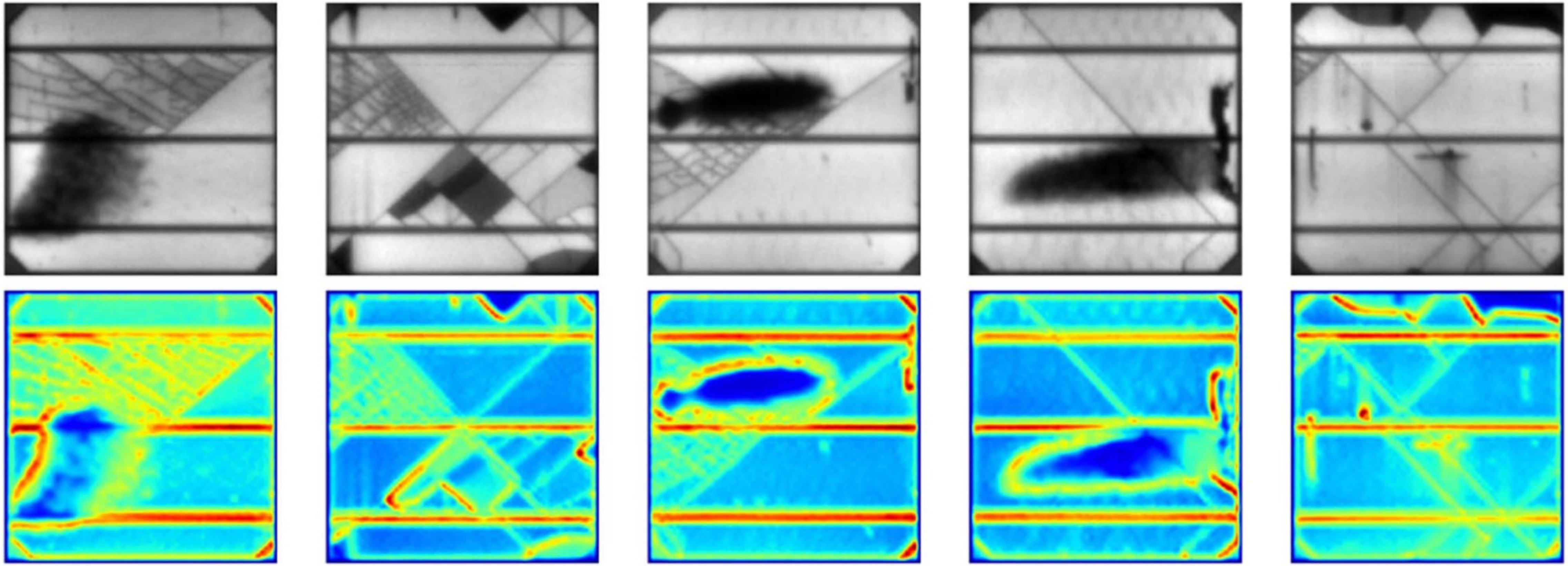

Absolute defective

Detection performance

5-fold cross validation

Average Maximum

Task	Model	Precision	Recall	F1-score	AUROC
Task-A	Rule	0.836 (0.982) → 0.871 (1.000)	0.954 (0.983) → 0.959 (1.000)	0.888 (0.956) → 0.906 (0.969)	**0.874 (0.984) → 0.880 (0.990)**
	DT	0.743 (1.000) → 0.726 (0.919)	0.753 (0.935) → 0.842 (1.000)	0.726 (0.840) → 0.774 (0.919)	**0.815 (0.901) → 0.820 (0.951)**
	RF	0.752 (0.938) → 0.796 (0.922)	0.909 (0.984) → 0.874 (1.000)	0.817 (0.961) → 0.820 (0.939)	**0.831 (0.997) → 0.870 (0.973)**
	XGB	0.694 (0.922) → 0.821 (0.978)	0.945 (0.983) → 0.771 (1.000)	0.790 (0.937) → 0.788 (0.925)	**0.817 (0.992) → 0.844 (0.964)**
	LGBM	0.688 (0.827) → 0.754 (0.979)	0.945 (1.000) → 0.900 (1.000)	0.789 (0.905) → 0.784 (0.887)	**0.813 (0.981) → 0.829 (0.949)**
	SVM	0.557 (0.915) → 0.624 (0.873)	0.958 (1.000) → 0.916 (1.000)	0.675 (0.893) → 0.733 (0.932)	0.748 (0.914) → 0.728 (0.962)
	EffNetB0	0.614 (0.846)	0.869 (0.984)	0.694 (0.846)	0.796 (0.937)
	L-CNN [17]	- (0.904)	- (0.954)	- (0.929)	- (0.934)
	DFB-SVM [17]	- (0.948)	- (0.974)	- (0.961)	- (0.979)
Task-B	Rule	0.816 (0.946) → 0.803 (0.929)	0.870 (0.967) → 0.881 (0.992)	0.839 (0.926) → 0.825 (0.905)	**0.851 (0.963) → 0.855 (0.929)**
	DT	0.696 (0.843) → 0.719 (0.752)	0.888 (0.991) → 0.931 (0.974)	0.771 (0.835) → 0.811 (0.848)	**0.748 (0.866) → 0.794 (0.891)**
	RF	0.751 (0.954) → 0.752 (0.888)	0.833 (0.957) → 0.908 (1.000)	0.773 (0.875) → 0.815 (0.892)	**0.790 (0.872) → 0.812 (0.943)**
	XGB	0.691 (0.810) → 0.752 (0.859)	0.916 (1.000) → 0.889 (0.991)	0.781 (0.888) → 0.809 (0.875)	**0.778 (0.899) → 0.801 (0.914)**
	LGBM	0.662 (0.801) → 0.708 (0.861)	0.951 (1.000) → 0.929 (1.000)	0.775 (0.890) → 0.797 (0.879)	**0.789 (0.905) → 0.791 (0.927)**
	SVM	0.684 (0.871) → 0.563 (0.784)	0.811 (1.000) → 0.984 (1.000)	0.715 (0.761) → 0.707 (0.854)	**0.656 (0.774) → 0.666 (0.862)**
	EffNetB0	0.594 (0.745)	0.938 (1.000)	0.719 (0.752)	0.642 (0.831)
	L-CNN [17]	- (0.807)	- (0.916)	- (0.858)	- (0.935)
	DFB-SVM [17]	- (0.879)	- (0.966)	- (0.916)	- (0.970)

Detection performance

Original image Attention map

Task	Model	Precision	Recall	F1-score	AUROC
Task-A	Rule	0.836 (0.982) → 0.871 (1.000)	0.954 (0.983) → 0.959 (1.000)	0.888 (0.956) → 0.906 (0.969)	**0.874 (0.984) → 0.880 (0.990)**
	DT	0.743 (1.000) → 0.726 (0.919)	0.753 (0.935) → 0.842 (1.000)	0.726 (0.840) → 0.774 (0.919)	**0.815 (0.901) → 0.820 (0.951)**
	RF	0.752 (0.938) → 0.796 (0.922)	0.909 (0.984) → 0.874 (1.000)	0.817 (0.961) → 0.820 (0.939)	**0.831 (0.997) → 0.870 (0.973)**
	XGB	0.694 (0.922) → 0.821 (0.978)	0.945 (0.983) → 0.771 (1.000)	0.790 (0.937) → 0.788 (0.925)	**0.817 (0.992) → 0.844 (0.964)**
	LGBM	0.688 (0.827) → 0.754 (0.979)	0.945 (1.000) → 0.900 (1.000)	0.789 (0.905) → 0.784 (0.887)	**0.813 (0.981) → 0.829 (0.949)**
	SVM	0.557 (0.915) → 0.624 (0.873)	0.958 (1.000) → 0.916 (1.000)	0.675 (0.893) → 0.733 (0.932)	0.748 (0.914) → 0.728 (0.962)
	EffNetB0	0.614 (0.846)	0.869 (0.984)	0.694 (0.846)	0.796 (0.937)
	L-CNN [17]	- (0.904)	- (0.954)	- (0.929)	- (0.934)
	DFB-SVM [17]	- (0.948)	- (0.974)	- (0.961)	- (0.979)
Task-B	Rule	0.816 (0.946) → 0.803 (0.929)	0.870 (0.967) → 0.881 (0.992)	0.839 (0.926) → 0.825 (0.905)	**0.851 (0.963) → 0.855 (0.929)**
	DT	0.696 (0.843) → 0.719 (0.752)	0.888 (0.991) → 0.931 (0.974)	0.771 (0.835) → 0.811 (0.848)	**0.748 (0.866) → 0.794 (0.891)**
	RF	0.751 (0.954) → 0.752 (0.888)	0.833 (0.957) → 0.908 (1.000)	0.773 (0.875) → 0.815 (0.892)	**0.790 (0.872) → 0.812 (0.943)**
	XGB	0.691 (0.810) → 0.752 (0.859)	0.916 (1.000) → 0.889 (0.991)	0.781 (0.888) → 0.809 (0.875)	**0.778 (0.899) → 0.801 (0.914)**
	LGBM	0.662 (0.801) → 0.708 (0.861)	0.951 (1.000) → 0.929 (1.000)	0.775 (0.890) → 0.797 (0.879)	**0.789 (0.905) → 0.791 (0.927)**
	SVM	0.684 (0.871) → 0.563 (0.784)	0.811 (1.000) → 0.984 (1.000)	0.715 (0.761) → 0.707 (0.854)	**0.656 (0.774) → 0.666 (0.862)**
	EffNetB0	0.594 (0.745)	0.938 (1.000)	0.719 (0.752)	0.642 (0.831)
	L-CNN [17]	- (0.807)	- (0.916)	- (0.858)	- (0.935)
	DFB-SVM [17]	- (0.879)	- (0.966)	- (0.916)	- (0.970)

Detection performance

Task	Model	Precision	Recall	F1-score	AUROC
Task-A	Rule	0.836 (0.982) → 0.871 (1.000)	0.954 (0.983) → 0.959 (1.000)	0.888 (0.956) → 0.906 (0.969)	**0.874 (0.984) → 0.880 (0.990)**
	DT	0.743 (1.000) → 0.726 (0.919)	0.753 (0.935) → 0.842 (1.000)	0.726 (0.840) → 0.774 (0.919)	**0.815 (0.901) → 0.820 (0.951)**
	RF	0.752 (0.938) → 0.796 (0.922)	0.909 (0.984) → 0.874 (1.000)	0.817 (0.961) → 0.820 (0.939)	**0.831 (0.997) → 0.870 (0.973)**
	XGB	0.694 (0.922) → [illegible]	[illegible]	[illegible]88 (0.925)	**0.817 (0.992) → 0.844 (0.964)**
	LGBM	0.688 (0.827) → [illegible]	[illegible]	[illegible]84 (0.887)	**0.813 (0.981) → 0.829 (0.949)**
	SVM	0.557 (0.915) → [illegible]	[illegible]	[illegible]33 (0.932)	0.748 (0.914) → 0.728 (0.962)
	EffNetB0	0.614 [illegible]	[illegible]	[illegible]	0.796 (0.937)
	L-CNN [17]	- (0[illegible]	[illegible]	[illegible]	- (0.934)
	DFB-SVM [17]	- (0[illegible]	[illegible]	[illegible]	- (0.979)
Task-B	Rule	0.816 (0.946) → [illegible]	[illegible]	[illegible]25 (0.905)	**0.851 (0.963) → 0.855 (0.929)**
	DT	0.696 (0.843) → [illegible]	[illegible]	[illegible]11 (0.848)	**0.748 (0.866) → 0.794 (0.891)**
	RF	0.751 (0.954) → [illegible]	[illegible]	[illegible]15 (0.892)	**0.790 (0.872) → 0.812 (0.943)**
	XGB	0.691 (0.810) → [illegible]	[illegible]	[illegible]09 (0.875)	**0.778 (0.899) → 0.801 (0.914)**
	LGBM	0.662 (0.801) → [illegible]	[illegible]	[illegible]97 (0.879)	**0.789 (0.905) → 0.791 (0.927)**
	SVM	0.684 (0.871) → [illegible]	[illegible]	[illegible]07 (0.854)	**0.656 (0.774) → 0.666 (0.862)**
	EffNetB0	0.594 (0.745)	0.938 (1.000)	0.719 (0.752)	0.642 (0.831)
	L-CNN [17]	- (0.807)	- (0.916)	- (0.858)	- (0.935)
	DFB-SVM [17]	- (0.879)	- (0.966)	- (0.916)	- (0.970)

0.874 (0.984) → 0.880 (0.990)
0.815 (0.901) → 0.820 (0.951)
0.831 (0.997) → 0.870 (0.973)
0.817 (0.992) → 0.844 (0.964)
0.813 (0.981) → 0.829 (0.949)

Detection performance

Task	Model	Precision	Recall	F1-score	AUROC
Task-A	Rule	0.836 (0.982) → 0.871 (1.000)	0.954 (0.983) → 0.959 (1.000)	0.888 (0.956) → 0.906 (0.969)	**0.874 (0.984) → 0.880 (0.990)**
	DT	0.743 (1.000) → 0.726 (0.919)	0.753 (0.935) → 0.842 (1.000)	0.726 (0.840) → 0.774 (0.919)	**0.815 (0.901) → 0.820 (0.951)**
	RF	0.752 (0.938) → [illegible]	[illegible]	[illegible] (0.939)	**0.831 (0.997) → 0.870 (0.973)**
	XGB	0.694 (0.922) → [illegible]	[illegible]	[illegible] (0.925)	**0.817 (0.992) → 0.844 (0.964)**
	LGBM	0.688 (0.827) → [illegible]	[illegible]	[illegible] (0.887)	**0.813 (0.981) → 0.829 (0.949)**
	SVM	0.557 (0.915) → [illegible]	[illegible]	[illegible] (0.932)	0.748 (0.914) → 0.728 (0.962)
	EffNetB0	0.614 [illegible]	[illegible]	[illegible]	0.796 (0.937)
	L-CNN [17]	- [illegible]	[illegible]	[illegible]	- (0.934)
	DFB-SVM [17]	- [illegible]	[illegible]	[illegible]	- (0.979)
Task-B	Rule	0.816 (0.946) → [illegible]	[illegible]	[illegible] (0.905)	**0.851 (0.963) → 0.855 (0.929)**
	DT	0.696 (0.843) → [illegible]	[illegible]	[illegible] (0.848)	**0.748 (0.866) → 0.794 (0.891)**
	RF	0.751 (0.954) → [illegible]	[illegible]	[illegible] (0.892)	**0.790 (0.872) → 0.812 (0.943)**
	XGB	0.691 (0.810) → [illegible]	[illegible]	[illegible] (0.875)	**0.778 (0.899) → 0.801 (0.914)**
	LGBM	0.662 (0.801) → [illegible]	[illegible]	[illegible] (0.879)	**0.789 (0.905) → 0.791 (0.927)**
	SVM	0.684 (0.871) → [illegible]	[illegible]	[illegible] (0.854)	**0.656 (0.774) → 0.666 (0.862)**
	EffNetB0	0.594 [illegible]	[illegible]	[illegible]	0.642 (0.831)
	L-CNN [17]	- (0.807)	- (0.916)	- (0.858)	- (0.935)
	DFB-SVM [17]	- (0.879)	- (0.966)	- (0.916)	- (0.970)

0.851 (0.963) → 0.855 (0.929)
0.748 (0.866) → 0.794 (0.891)
0.790 (0.872) → 0.812 (0.943)
0.778 (0.899) → 0.801 (0.914)
0.789 (0.905) → 0.791 (0.927)
0.656 (0.774) → 0.666 (0.862)

Detection performance

	Decision Tree (Simple machine learning)		Needs large-scale dataset EfficientNet-B0 (SOTA deep learning)
Task-A	0.820 (0.951)	>	0.796 (0.937)
Task-B	0.794 (0.891)	>	0.642 (0.831)

Training and inference efficiency

$2.696{\times}10^{-3}$ sec for feature extraction

Second	**Model**	**Training**	**Inference**
CPU	Rule	8.367×10^{-2}	3.609×10^{-6}
	DT	3.897×10^{-3}	1.071×10^{-5}
	RF	1.568×10^{-1}	8.135×10^{-5}
	XGB	3.643×10^{-2}	1.935×10^{-5}
	LGBM	4.681×10^{-2}	2.917×10^{-6}
	SVM	6.197×10^{-2}	2.796×10^{-5}
	EffNetB0	8.960×10^{2}	2.863×10^{-2}
GPU	EffNetB0	6.654×10^{1}	9.086×10^{-3}

Training and inference efficiency

2.696×10^{-3} sec for feature extraction

Second	Model	Training	Inference
CPU	Rule	8.367×10^{-2}	3.609×10^{-6}
	DT	$\boxed{3.897\times10^{-3}}$	1.071×10^{-5}
	RF	1.568×10^{-1}	8.135×10^{-5}
	XGB	3.643×10^{-2}	1.935×10^{-5}
	LGBM	4.681×10^{-2}	2.917×10^{-6}
	SVM	6.197×10^{-2}	2.796×10^{-5}
	EffNetB0	$\boxed{8.960\times10^{2}}$	2.863×10^{-2}
GPU	EffNetB0	6.654×10^{1}	9.086×10^{-3}

× 230k

Training and inference efficiency

2.696×10^{-3} sec for feature extraction

Second	Model	Training	Inference
CPU	Rule	8.367×10^{-2}	3.609×10^{-6}
	DT	3.897×10^{-3}	$\boxed{1.071 \times 10^{-5}}$
	RF	1.568×10^{-1}	8.135×10^{-5}
	XGB	3.643×10^{-2}	1.935×10^{-5}
	LGBM	4.681×10^{-2}	2.917×10^{-6}
	SVM	6.197×10^{-2}	2.796×10^{-5}
	EffNetB0	8.960×10^{2}	$\boxed{2.863 \times 10^{-2}}$
GPU	EffNetB0	6.654×10^{1}	9.086×10^{-3}

× 3k

Experiment on another dataset [12]

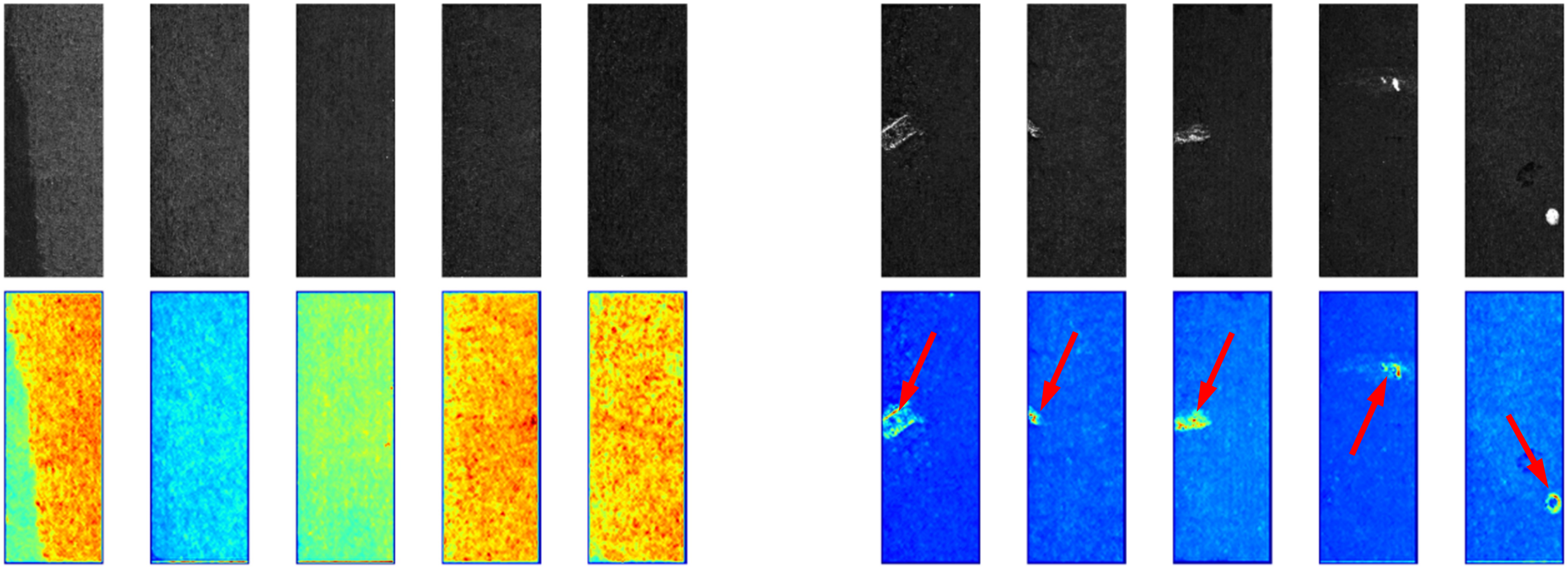

Non-defective

Defective

[12] J. Božič et al., "Mixed supervision for surface- defect detection: From weakly to fully supervised learning," *Computers in Industry*, 2021.

Experiment on another dataset [12]

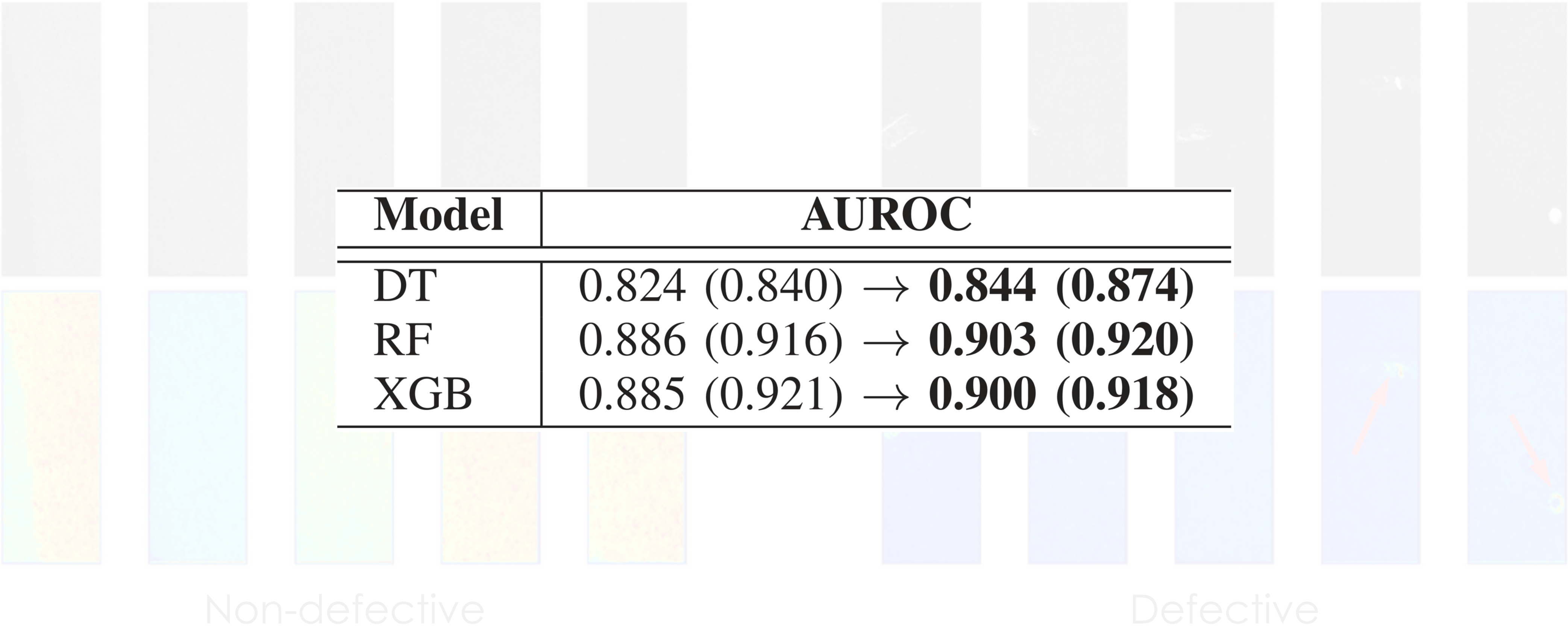

Model	AUROC
DT	0.824 (0.840) → **0.844 (0.874)**
RF	0.886 (0.916) → **0.903 (0.920)**
XGB	0.885 (0.921) → **0.900 (0.918)**

[12] J. Božič et al., “Mixed supervision for surface- defect detection: From weakly to fully supervised learning,” *Computers in Industry*, 2021.

Conclusions

- Simple yet powerful method for a real world problem
  - Attention mechanism recycling with 13 statistical features
  - Outperforms SOTA defect detection
  - Serves the purpose of sustainable green energy

- Applicable to other visual inspections
  - Surface defect detection in steel, film manufacturing, etc.

Future works

- Analysis of attention dependency on
  - Training dataset and
  - Neural network structure
- Attention recycling combined anomaly detection
  - Unsupervised anomaly detection
  - Cost-effective training strategy